astrocyte dysfunction followed by demyelination. Acta Neuropathol 120: 223–236.
32. Choi JW, Gardell SE, Herr DR, Rivera R, Lee CW, et al. (2011) FTY720 (fingolimod) efficacy in an animal model of multiple sclerosis requires astrocyte sphingosine 1-phosphate receptor 1 (S1P1) modulation. Proc Natl Acad Sci U S A 108: 751–756.
33. Naismith RT, Xu J, Tutlam NT, Scully PT, Trinkaus K, et al. (2010) Increased diffusivity in acute multiple sclerosis lesions predicts risk of black hole. Neurology 74: 1694–1701.
34. Sahraian MA, Radue EW, Haller S, Kappos L (2010) Black holes in multiple sclerosis: definition, evolution, and clinical correlations. Acta Neurol Scand 122: 1–8.
35. Blinkenberg M, Rune K, Jensen CV, Ravnborg M, Kyllingsbaek S, et al. (2000) Cortical cerebral metabolism correlates with MRI lesion load and cognitive dysfunction in MS. Neurology 54: 558–564.
36. Vercellino M, Merola A, Piacentino C, Votta B, Capello E, et al. (2007) Altered glutamate reuptake in relapsing-remitting and secondary progressive multiple sclerosis cortex: correlation with microglia infiltration, demyelination, and neuronal and synaptic damage. J Neuropathol Exp Neurol 66: 732–739.
37. Hyder F, Patel AB, Gjedde A, Rothman DL, Behar KL, et al. (2006) Neuronal-glial glucose oxidation and glutamatergic-GABAergic function. J Cereb Blood Flow Metab 26: 865–877.
38. Wang D, Ayers MM, Catmull DV, Hazelwood LJ, Bernard CC, et al. (2005) Astrocyte-associated axonal damage in pre-onset stages of experimental autoimmune encephalomyelitis. Glia 51: 235–240.
39. Van den Berg CJ, Mela P, Waelsch H (1966) On the contribution of the tricarboxylic acid cycle to the synthesis of glutamate, glutamine and aspartate in brain. Biochem Biophys Res Commun 23: 479–484.
40. Wyss MT, Magistretti PJ, Buck A, Weber B (2011) Labeled acetate as a marker of astrocytic metabolism. J Cereb Blood Flow Metab 31: 1668–1674.

Tada et al. Journal of Neuroinflammation 2014, 11:179
http://www.jneuroinflammation.com/content/11/1/179

JNI JOURNAL OF NEUROINFLAMMATION

SHORT REPORT Open Access

Partial suppression of M1 microglia by Janus kinase 2 inhibitor does not protect against neurodegeneration in animal models of amyotrophic lateral sclerosis

Satoru Tada[1,2], Tatsusada Okuno[1*], Yasumichi Hitoshi[3], Teruhito Yasui[2], Josephe Archie Honorat[1], Kazushiro Takata[1], Toru Koda[1], Hiroshi Shimagami[1], Choong Chi-Jing[1], Akiko Namba[1], Tomoyuki Sugimoto[4], Saburo Sakoda[5], Hideki Mochizuki[1], Hitoshi Kikutani[2] and Yuji Nakatsuji[1*]

Abstract

Background: Accumulating evidence has shown that the inflammatory process participates in the pathogenesis of amyotrophic lateral sclerosis (ALS), suggesting a therapeutic potential of anti-inflammatory agents. Janus kinase 2 (JAK2), one of the key molecules in inflammation, transduces signals downstream of various inflammatory cytokines, and some Janus kinase inhibitors have already been clinically applied to the treatment of inflammatory diseases. However, the efficacy of JAK2 inhibitors in treatment of ALS remains to be demonstrated. In this study, we examined the role of JAK2 in ALS by administering a selective JAK2 inhibitor, R723, to an animal model of ALS (mSOD1^{G93A} mice).

Findings: Orally administered R723 had sufficient access to spinal cord tissue of mSOD1^{G93A} mice and significantly reduced the number of *Ly6c positive* blood monocytes, as well as the expression levels of IFN-γ and nitric oxide synthase 2, inducible (iNOS) in the spinal cord tissue. R723 treatment did not alter the expression levels of Il-1β, Il-6, TNF, and NADPH oxidase 2 (NOX2), and suppressed the expression of Retnla, which is one of the markers of neuroprotective M2 microglia. As a result, R723 did not alter disease progression or survival of mSOD1^{G93A} mice.

Conclusions: JAK2 inhibitor was not effective against ALS symptoms in mSOD1^{G93A} mice, irrespective of suppression in several inflammatory molecules. Simultaneous suppression of *anti-inflammatory microglia* with a failure to inhibit critical other inflammatory molecules might explain this result.

Keywords: Amyotrophic lateral sclerosis, SOD1-G93A transgenic mice, R723, Janus kinase 2, JAK2 inhibitor, Neuroinflammation, Interferon gamma, M1/M2 microglia

Findings

Introduction

Amyotrophic lateral sclerosis (ALS) is a devastating disease characterized by progressive degeneration of motor neurons in the brain and spinal cord, resulting in muscle weakness. Although the precise mechanism of ALS remains unknown, inflammatory microglial activation plays an important role in pathogenesis [1-3]. The inflammatory molecule IFN-γ, which is primarily produced by Th1 lymphocytes and is a potent activating factor for inflammatory M1 microglia, contributes to the loss of motor neurons in ALS [4,5]. Furthermore, a recent report showed that Ly6c-high inflammatory monocytes are recruited to the spinal cord in mSOD1^{G93A} mice, and that treatment with anti-Ly6c monoclonal antibodies reduces monocyte recruitment to the spinal cord and ameliorates neurodegeneration in these animals [6].

Janus kinases (JAKs) are centrally implicated in cytokine receptor-mediated cell signaling pathways, which drive a

* Correspondence: okuno@neurol.med.osaka-u.ac.jp; yuji@neurol.med.osaka-u.ac.jp
[1]Department of Neurology, Osaka University Graduate School of Medicine, 2-2 Yamadaoka, Suita, Osaka 565-0871, Japan
Full list of author information is available at the end of the article

range of myeloid malignancies [7] as well as inflammatory diseases [8]. The JAK family member JAK2 is responsible for transducing signals for several proinflammatory cytokines including IFN-γ and Il-12, as well as for differentiation of myeloid cells [9]. In an animal model of rheumatoid arthritis (RA) and experimental autoimmune encephalitis (EAE), suppression of the JAK pathway ameliorated disease severity by suppressing Th1 cells and deactivating monocytes [10,11]. A growing number of JAK inhibitors have been developed and clinically applied to the treatment of various inflammatory disease including RA, psoriasis, and inflammatory bowel disease [12-14]. Although activators of JAK2 such as IFN-γ, Il-6, and Il-12 are reported to be implicated in ALS pathogenesis [3], the role of JAK2 in the ALS-related neuroinflammation remains totally unknown.

Based on these findings, we hypothesized that JAK2 inhibition could ameliorate neurodegeneration in ALS model mice by inhibiting harmful inflammatory processes in microglia/macrophages. To test this idea, we treated transgenic mice overexpressing the familial ALS-associated G93A SOD1 mutation (mSOD1^{G93A} mice) with R723, an orally active inhibitor of JAK2 [15].

Methods

Ethics statements

All animal experiments were conducted in accordance with the guidelines of Osaka University, which specifically approved this study (Permit number: Biken-AP-H21-28-0).

RNA extraction and RT-qPCR analysis

Spinal cord tissues were collected from mSOD1^{G93A} mice and total mRNA and cDNA were generated as previously described [1]. The synthesized cDNA was amplified using SYBR Premix Ex Taq II (for TNF, MCP1, Il-12b, iNOS, Il-6, Il-1b, NOX2, Ly6c, Arg1, Ym1, Il-4, EPO, CSF3 and Retnla) (Takara Bio Inc., Otsu, Japan) or TaqMan Gene Expression Assays (for IFN-γ, Il-6, Il-12a and GM-CSF) (Applied Biosystems, Foster City, CA, USA) and analyzed as previously described [1].

Immunohistochemistry

Spinal cord sections of mSOD1^{G93A} mice were prepared as previously described [1]. The following antibodies were used: rabbit anti-JAK2 (phospho Y1007 + Y1008) monoclonal antibody (1:200; Abcam, Cambridge, UK), rabbit anti-iNOS polyclonal antibody (1:50; BD Biosciences, Franklin Lakes, NJ, USA) and Alexa Fluor 488°-conjugated mouse anti-glial fibrillary acidic protein (GFAP) monoclonal antibody (1:200; Cell Signaling Technology, Beverly, MA, USA). The following secondary antibodies were applied: Cy5-conjugated F(ab') 2 fragment donkey anti-rabbit IgG (1:500; Jackson ImmunoResearch Laboratories, West Grove, PA, USA).

Animals and R723 administration

mSOD1^{G93A} mice were obtained from The Jackson Laboratory and backcrossed with C57BL/6 mice for at least 10 generations. R723 was administered by oral gavage starting on day 90. For the analysis of motor function by rotarod test, weight measurement, and survival, R723 dosing continued until day 120 (70 mg/kg twice daily; 5 days on, 2 days off). To evaluate *in vivo* pharmacokinetics, plasma and spinal cord tissues were collected at 0.5, 1, 2, and 4 hours post-dose, and R723 levels in plasma and spinal cord tissue were determined by LC/MS/MS.

Flow cytometry of peripheral blood cells

Peripheral blood cells were collected from mSOD1^{G93A} mice on day 4 post-dose. The following antibodies were used: APC-Cy7-labeled anti-CD11b (M1/70; BioLegend, San Diego, CA, USA) and fluorescein isothiocyanate (FITC)-labeled anti-Ly6c (HK1.4; BioLegend, San Diego, CA, USA). Flow cytometry was performed using a FACS Canto™ II with the Diva ™ software (Becton Dickinson, Franklin Lakes, NJ, USA). Acquired data were analyzed using the FlowJo software (Tree Star, Inc., Ashland, OR, USA).

Lectin staining

Sections were permeabilized with 0.2% tris-buffered saline with tween (TBST) for 10 minutes and then incubated with FITC-conjugated tomato (*Lycopersicon esculentum*) lectin (Sigma-Aldrich, St Louis, MO, USA) diluted 1:750 in PBS overnight at 4°C. The sections were washed ×3 in 0.2% TBST for 5 minutes and mounted with VECTASHIELD Mounting Medium containing 4',6-diamidino-2-phenylindole (DAPI) (Vector Laboratories, Burlingame, CA, USA). The fluorescently labeled sections were examined using a LSM 510 confocal microscope (Carl Zeiss Microscopy, Jena, Germany).

Nissl staining

Spinal cord sections of mSOD1^{G93A} mice were prepared as previously described [1]. Every fifth section was collected and stained with cresyl violet.

Statistics

Data are expressed as means ± SEM. Differences in animal weight measurements and rotarod tests were assessed using analysis of variance (ANOVA). Statistical significance in survival experiments was determined using Kaplan-Meier survival statistics. Statistical significance in all other experiments was assessed using the Mann-Whitney *U*-test. $P < 0.05$ was considered statistically significant.

Results

To confirm whether expression of inflammatory cytokines was upregulated in the spinal cords of late-stage mSOD1^{G93A} mice, we evaluated spinal cord mRNA expression of several genes encoding inflammatory molecules. Consistent with a previous report [16], RT-qPCR analysis revealed that the expression levels of IFN-γ, Il-6, Il-12a, and granulocyte macrophage colony-stimulating factor (GM-CSF) increased along with disease progression (Figure 1A and Additional file 1: Supplementary information). In addition, microglia in the spinal cords of late stage mSOD1^{G93A} mice (130 days old) had enhanced phosphorylation of JAK2 compared with pre-onset stage mSOD1^{G93A} mice (70 days old), providing a therapeutic rationale for JAK2 inhibition against ALS (Figure 1B, C).

To investigate the role of JAK2 pathway in ALS, we used R723, which is a selective small-molecule JAK2 inhibitor originally developed by Rigel Pharmaceuticals Inc, (San Francisco, CA, USA) for the treatment of myeloproliferative neoplasms such as polycythemia vera, essential

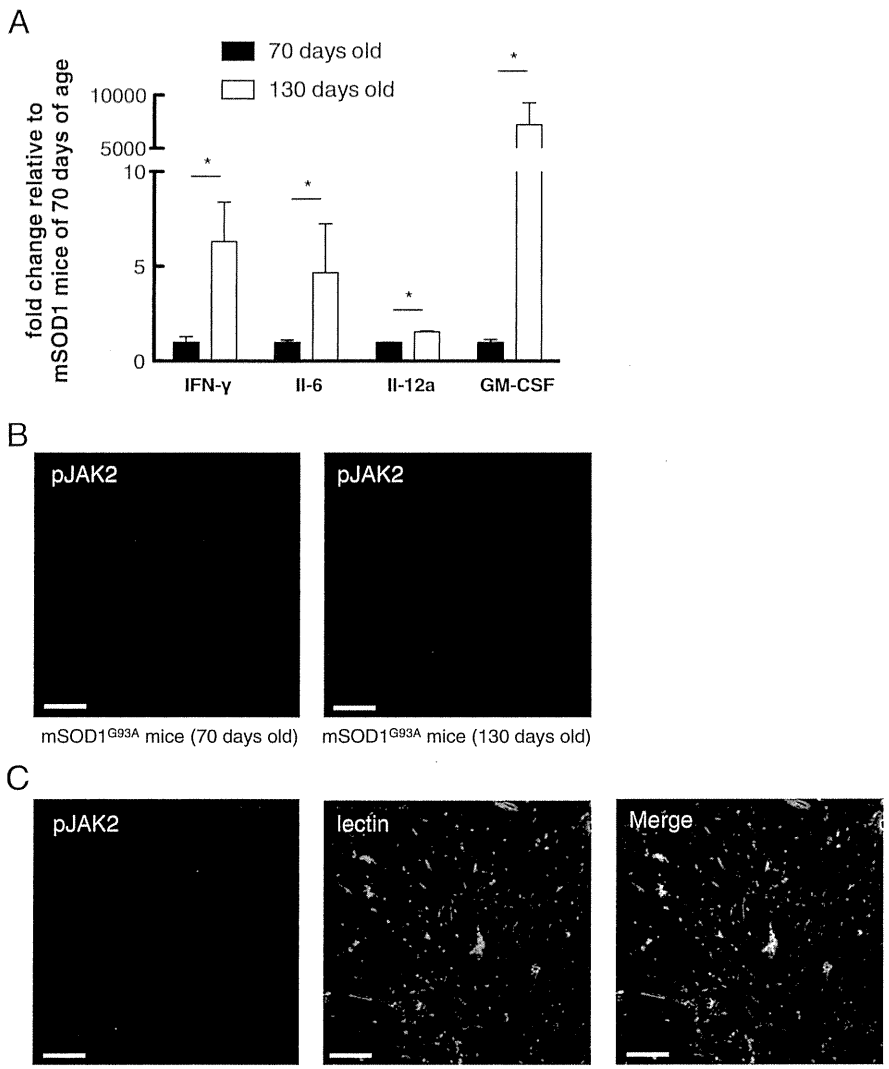

Figure 1 Enhanced phosphorylation of Janus kinase 2 (JAK2) and up-regulation of JAK2-related genes in the spinal cord of mSOD1^{G93A} mice in the late stage of disease. (A) Quantitative RT-PCR analyses of spinal cords of mSOD1^{G93A} mice (70 days and 130 days old) were performed (n = 3 to 4 for each group). Expression levels of IFN-γ, Il-6, Il-12a, and GM-CSF were significantly elevated in 130-day-old mSOD1^{G93A} mice relative to those in 70-day-old mice. Data are expressed as means ± SEM. *$P < 0.05$, Mann-Whitney *U*-test. **(B)** Immunohistochemical analysis showed enhanced phosphorylation of JAK2 in the spinal cord of late-stage mSOD1^{G93A} mouse compared with the spinal cord of pre-onset-stage mSDO1 mouse. Scale bar = 100 μm. Data are representative of three animals. **(C)** Sections of 130-day-old mSOD1^{G93A} mouse spinal cord were co-stained with Cy5-conjugated anti-phosphorylated JAK2 antibodies and FITC-conjugated tomato lectin. Scale bar = 100 μm. Data are representative of three animals.

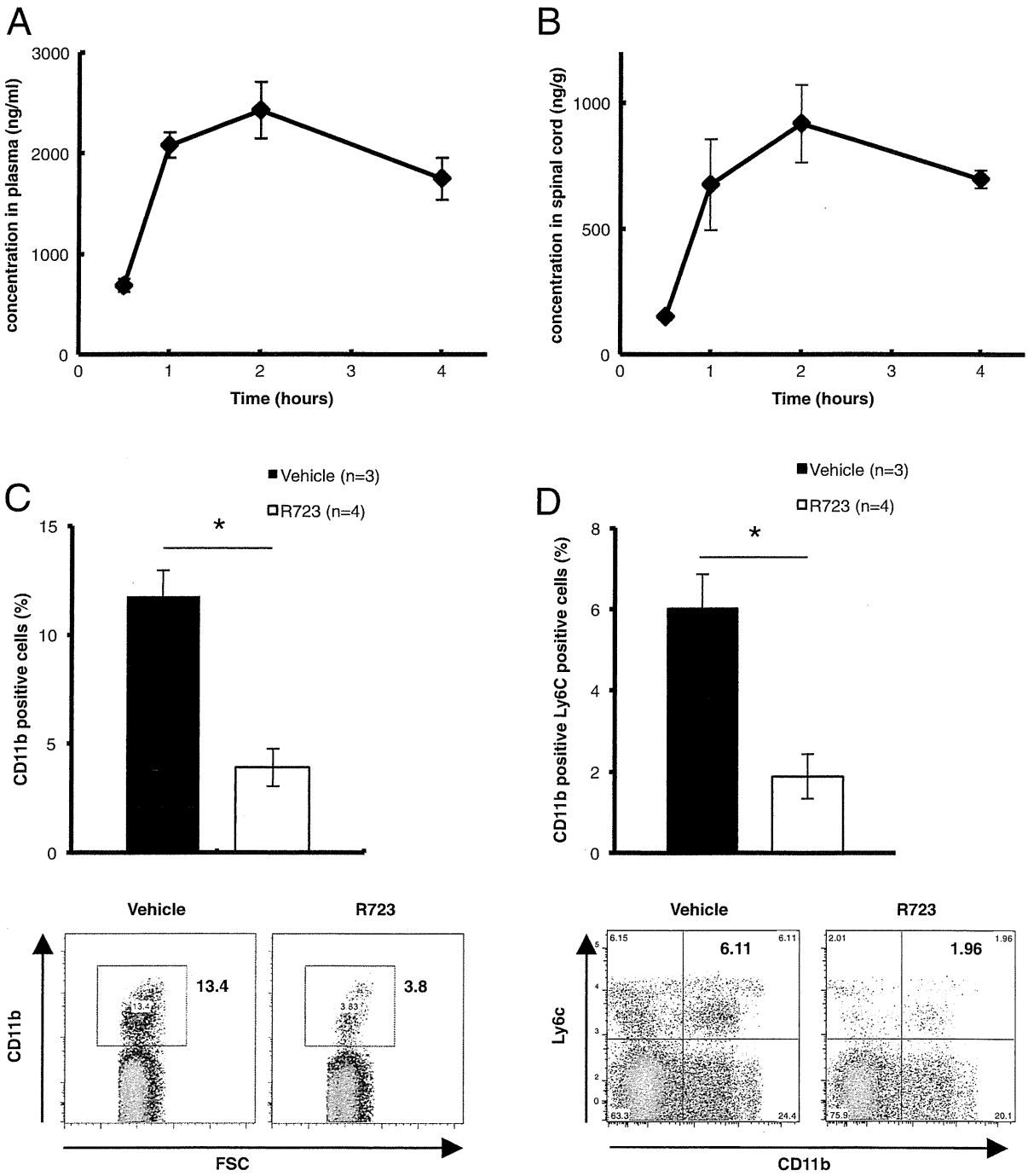

Figure 2 Pharmacological properties of R723 and its effects on peripheral monocytes. (A, B) Pharmacological profile of R723 in plasma and spinal cord tissue after single-dose administration by oral gavage to 120-day-old female mSOD1^{G93A} mice. Concentration of the compound at the indicated time points was quantified by LC/MS/MS assay. **(C, D)** Effects of R723 treatment on the proportion of CD11b + or Ly6c + cells in peripheral blood. mSOD1^{G93A} mice (120 days old) were orally administered with vehicle or R723 (70 mg/kg) for 4 days. Blood were harvested, and the proportions of CD11b + and Ly6c + cells were evaluated by FACS. **(C)** The proportion of CD11b + monocytes was significantly reduced in peripheral blood of R723-treated mSOD1^{G93A} mice. **(D)** Four-day treatment with R723 reduced the proportion of Ly6c + CD11b + monocytes in peripheral blood. In panels **(C)** and **(D)**, n = 3 for vehicle-treated mice, and n = 4 for R723 treated mice. Data are expressed as means ± SEM. *$P < 0.05$, Mann-Whitney *U*-test.

thrombocythemia and primary myelofibrosis (Additional file 2: Figure S1A) [15]. First, to investigate the drug distribution, we administered R723 by oral gavage to mSOD1^{G93A} mice and measured concentrations of R723 in serum and spinal cord tissue. R723 had sufficient access to spinal cord tissue (Figure 2A, B) (spinal area under the curve (AUC) (0.5 to 4]/plasma AUC (0.5 to 4] ratio: 0.368) [17]. Next, we tested whether R723 treatment could deplete monocytes circulating in peripheral blood. After 4 days of treatment with R723, mSOD1^{G93A} mice

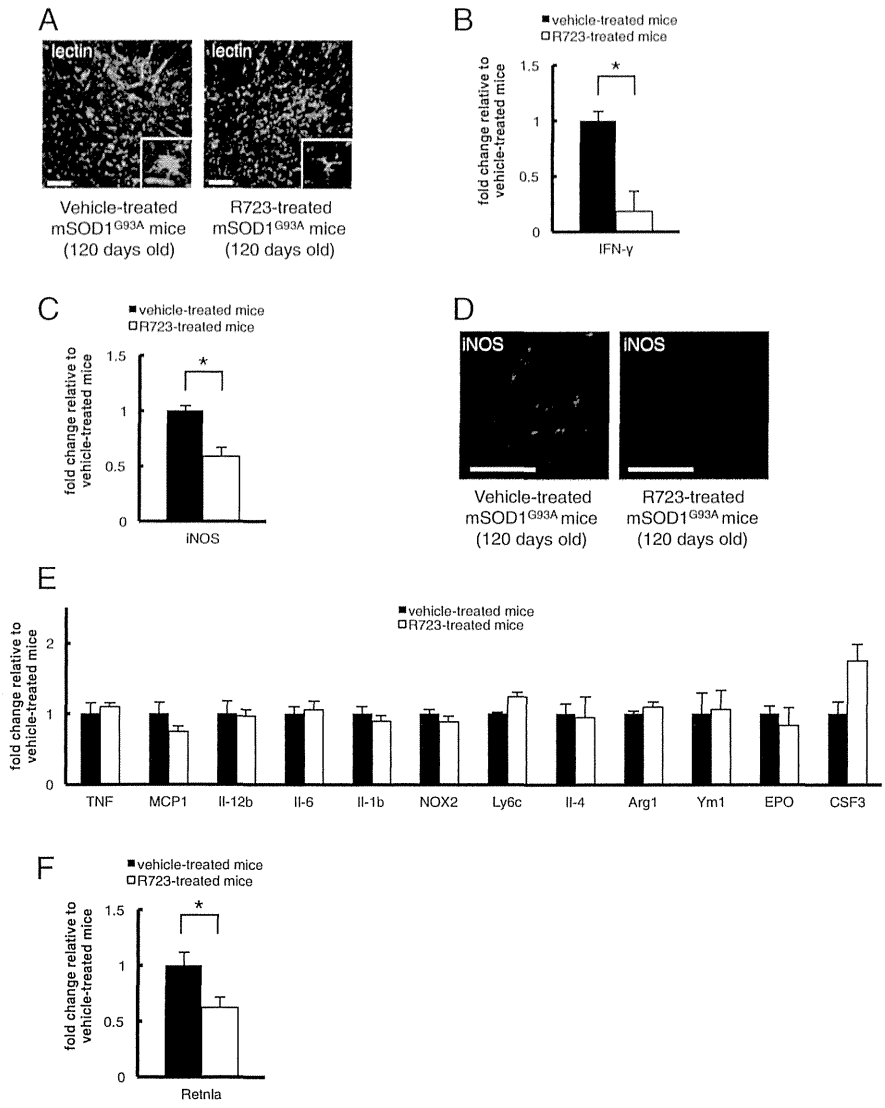

Figure 3 Effects of R723 on inflammation-related gene expression and microgliosis in spinal cord of mSOD1^{G93A} transgenic mice. (A) R723-treated mSOD1^{G93A} mice had reduced number of lectin-positive microglia in the spinal cord compared with vehicle-treated controls. Lumbar sections of the spinal cord were stained with fluorescein isothiocyanate (FITC)-conjugated tomato lectin. Scale bar = 100 μm. Data are representative of three animals. **(B, C)** Quantitative RT-PCR analyses in spinal cords of R723-treated mSOD1^{G93A} mice and vehicle-treated controls (120 days old) were performed (n = 4 in each group). The expression levels of IFN-γ and iNOS were significantly reduced in the R723-treated group ($P = 0.0495$ for each experiment). **(D)** Immunohistochemical analysis showed R723 treatment for 30 days had suppressed the expression level of iNOS in the spinal cords of mSOD1^{G93A} mice. Scale bar = 100 μm. Data are representative of three animals. **(E)** Quantitative RT-PCR analyses in spinal cords of R723 treated mSOD1^{G93A} mice and vehicle-treated controls (120 days old) were performed (n = 4 in each group). Relative mRNA expression is shown for TNF, MCP1, Il-12b, Il-6, Il-1b, NOX2, and Ly6c, which are related to M1 macrophages/microglia, and for Il-4, Arg1, Ym1, Il-4, EPO and CSF3, which are related to M2 macrophages/microglia. There were no significant differences in the expression levels of these molecules between two groups after the correction of multiple comparisons. **(F)** Quantitative RT-PCR analysis revealed that R723 had suppressed the expression of Retnla after 30 days of treatment in the spinal cords of mSOD1^{G93A} mice ($P = 0.0495$, n = 4 in each group). Data are expressed as means ± SEM. *$P < 0.05$, Mann-Whitney *U*-test.

had significantly fewer CD11b-positive cells and Ly6c-positive monocytes in peripheral blood (Figure 2C, D and Additional file 1: Supplementary information).

To further confirm the anti-inflammatory effect of R723, we evaluated the microgliosis and astrocytosis in spinal cord tissue of R723-treated mSOD1^{G93A} mice. Lectin staining revealed that R723 treatment had suppressed microgliosis in the spinal cords of mSOD1^{G93A} mice, although it did not affect astrocytosis (Figure 3A and Additional file 3: Figure S2A). In addition, we evaluated the mRNA expression of inflammation-related and M1/M2 microglia-related genes in spinal cord tissue of R723-treated mSOD1^{G93A} mice. Consistent with the anti-inflammatory effects of JAK2 inhibitor as previously reported [17], R723 treatment suppressed IFN-γ and iNOS expression dose-dependently, suggesting that the drug exerted anti-inflammatory effects in the spinal cords of mSOD1^{G93A} mice (Figure 3B, C and Additional file 4: Figure S3A). In addition, the effect of R723 against iNOS expression was confirmed by immunohistochemical analysis (Figure 3D). However, R723 had no obvious effects on other inflammatory molecules such as TNF, Il-12b, Il-6, Il-1β, and NOX2. Additionally, there was no significant difference between two groups in the spinal cord expression levels of monocyte chemotactic protein 1 (MCP1) and Ly6c, which are important for the migration and activation of inflammatory monocytes, as well as those of Il-4, arginase, liver (Arg1), chitinase-3-like 3 (Ym1), erythropoietin (EPO), and colony-stimulating factor 3 (CSF3), which are involved in the activation of M2 microglia (Figure 3E). Unexpectedly, R723 suppressed expression of resistin-like alpha (Retnla), a marker of anti-inflammatory M2 microglia, in spinal cord tissue of mSOD1^{G93A} mice after 30 days of treatment, although this effect was not evident after 5 days of treatment (Figure 3F and Additional file 4: Figure S3B). Collectively, these results suggest that oral administration of R723 decreased the number of Ly6c-positive monocytes in peripheral blood

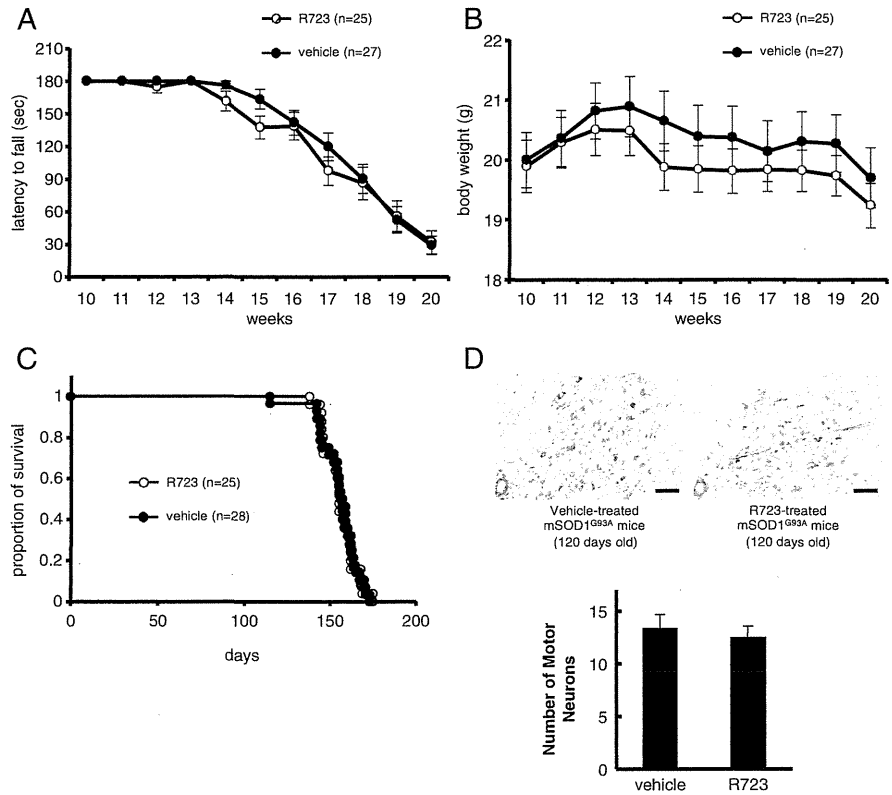

Figure 4 Body weight, motor performance, and survival of R723- or vehicle-treated mSOD1^{G93A} mice. (A) Time course of motor performance in the rotarod test. Performance of R723-treated (open circles, n = 25) and vehicle-treated (filled circles, n = 27) mSOD1^{G93A} mice were comparable. **(B)** Changes in mean body weight of R723-treated (n = 25) and vehicle-treated (n = 27) mSOD1 ^{G93A} mice. **(C)** Kaplan-Meier survival curve. R723 treatment did not affect the survival of mSOD1 ^{G93A} mice (R723-treated group, n = 25; vehicle-treated group, n = 28) (P = 0.964). **(D)** Nissl staining of transverse sections of lumbar spinal cord. Motor neurons were counted and statistical analysis is shown. Scale bar = 50 μm. Data are expressed as means ± SEM. Statistical analysis was performed using ANOVA **(A, B)**, log-rank test **(C)**, and the Mann-Whitney *U*-test.

and reduced the expression of several inflammatory genes in the spinal cords of mSOD1^{G93A} mice, leading to suppressed microglial activation.

Because R723 suppresses several pathways that seem to be harmful in ALS, we tested whether R723 could ameliorate neurodegeneration in mSOD1^{G93A} mice. Oral administration of R723 (70 mg/kg, twice daily; 5 days on, 2 days off) to mSOD1^{G93A} mice was started at 90 days of age and continued until 120 days of age. Motor performance was evaluated by rotarod test, and muscle atrophy was monitored by body weight reduction. Decline in motor performance of the R723-treated mSOD1^{G93A} mice was compared with that of the vehicle-treated littermates. Throughout the disease process, there was no significant change in rotarod performance or body weight between the two groups (Figure 4A, B) ($P > 0.05$ for each time point, ANOVA). Additionally, survival times for R723-treated and vehicle-treated mSOD1^{G93A} mice were comparable (Figure 4C) (average survival time; R723 treated group: 155.6 ± 1.8 days (n = 25); vehicle-treated group: 155.1 ± 2.2 days (n = 28), $P = 0.96$, log-rank test). Consistent with these observations, Nissl staining revealed that R723 treatment had led to unaltered motor neuron survival in the spinal cords of mSOD1^{G93A} mice in both groups (Figure 4D). Collectively, these results showed that R723 penetrated the spinal cord of mSOD1^{G93A} mice and suppressed inflammation, but did not affect neurodegeneration *in vivo*.

Discussion

In this study, we tried to suppress harmful inflammatory processes in mSOD1^{G93A} mice by treating them with a JAK2 inhibitor. Although R723 was effective in depleting Ly6c-positive monocytes and suppressing IFN-γ and iNOS expression in the spinal cord, the drug did not affect disease progression or survival of these mice.

We examined the expression levels of inflammation-related genes including *TNF, MCP1, Il-1β*, and *NOX2*, which play critical roles in the pathogenesis of ALS [3], and found that they were not reduced after JAK2 inhibition. It is possible that inflammation driven by these molecules masked the effects of reductions in IFN-γ and iNOS expression.

One explanation for the lack of a neuroprotective effect of R723 could be the suppression of Retnla, an M2 microglia-related gene. M2 microglial activation, which is driven by Il-4 and Il-13 produced by Th2 lymphocytes, exerts protective roles in ALS [3]. Recently, another group reported that JAK2 is activated after the recruitment of Il-13 to its receptor, and revealed that Il-13 utilizes the JAK2 signaling pathway [18]. Therefore, we speculate that suppression of Retnla counteracts the anti-inflammatory effects of R723, preventing it from exerting a neuroprotective effect *in vivo*.

Alternatively, R723 might have inhibited a neuroprotective effect of JAK2. There is a report that suggests JAK2 signaling is implicated in the prevention of neuronal apoptosis in traumatic brain injury [19].

In conclusion, R723 alone was not sufficient to protect against neurodegeneration in mSOD1^{G93A} mice, although it suppressed the expression of several proinflammatory molecules and depleted monocytes. Based on our results, it is possible that in order to ameliorate neurodegeneration in ALS, we need not only to suppress JAK2 mediated inflammation but also prevent other inflammatory pathways. Furthermore, we may need to activate neuroprotective M2 microglia to alleviate neurodegeneration in ALS.

Additional files

Additional file 1: Supplementary information. Immunohistochemical analysis of the spinal cord of mSOD1^{G93A} mice and flow cytometric analysis of the peripheral blood monocytes of mSOD1^{G93A} mice. (A) Sections of mSOD1^{G93A} mouse spinal cord were co-stained with FITC-conjugated anti-CD206 receptor antibodies and Cy5-conjugated anti–iNOS antibodies. Scale bar = 200 μm. (B) The number of Ly6c positive and CD11b positive blood monocyte remained unchanged along with the disease progression. Peripheral blood cells were collected from mSOD1^{G93A} mice (70 days old mice and 130 days old ones). The following antibodies were used: APC-Cy7–labeled anti-CD11b and FITC-labeled anti-Ly6c. Flow cytometry was performed using a FACS Canto™ II with the Diva ™ software and acquired data were analyzed using the FlowJo software.

Additional file 2: Figure S1. R723 is a selective small-molecule JAK2 inhibitor. (A) Chemical structure of R723 is shown.

Additional file 3: Figure S2. R723 had no effect on astrocytosis in the spinal cords of mSOD1^{G93A} mice. (A) The number of GFAP-positive astrocytes in the spinal cord did not differ between R723-treated mSOD1^{G93A} mice and vehicle-treated controls. Lumbar sections of the spinal cord were stained with Alexa Fluor 488®-conjugated anti-GFAP antibody. Scale bar =100 μm. Data are representative of three animals.

Additional file 4: Figure S3. R723 had a dose-dependent effect on the suppression of inflammation-related genes. (A) Quantitative RT-PCR analyses revealed that lower dose of R723 (17.5mg/kg, twice a day, 5 days on/2 days off regimen) did not change the expression profiles of IFN-γ, iNOS and Retnla in the spinal cords of mSOD1^{G93A} mice (n = 3 in lower dose group and n = 4 in other groups). (B) Quantitative RT-PCR analyses in spinal cords of R723-treated mSOD1^{G93A} mice and vehicle-treated controls were performed after 5 days of treatment (n = 3 in each group). The expression level of iNOS was significantly reduced in the R723-treated group ($P = 0.0495$). Data are expressed as means ± SEM. *$P < 0.05$, Mann-Whitney *U*-test.

Abbreviations

ALS: amyotrophic lateral sclerosis; ANOVA: analysis of variance; Arg1: arginase, liver; AUC: area under the curve; CSF3: colony-stimulating factor 3; DAPI: 4',6-diamidino-2-phenylindole; EAE: experimental autoimmune encephalitis; EPO: erythropoietin; FITC: fluorescein isothiocyanate; GFAP: glial fibrillary acidic protein; GM-CSF: granulocyte macrophage-colony stimulating factor; IFN: interferon; Il: interleukin; JAK2: Janus kinase 2; JAKs: Janus kinases; MCP1: monocyte chemotactic protein 1; NOX2: NADPH oxidase 2; PBS: phosphate-buffered saline; PCR: polymerase chain reaction; RA: rheumatoid arthritis; Retnla: resistin-like alpha; TBST: tris-buffered saline with tween; TNF: tumor necrosis factor; Ym1: chitinase-3-like 3; iNOS: nitric oxide synthase 2, inducible; mSOD1^{G93A} mice: transgenic mice overexpressing the familial ALS-associated G93A SOD1 mutation.

Competing interests

YH is an employee of Rigel Pharmaceuticals, Inc. The remaining authors declare that they have no competing interests.

Authors' contributions
ST designed, performed, and analyzed the experiments; coordinated collaborations; and wrote the manuscript. TO and YH performed and analyzed experiments. TY, HK, SS, and HM assisted in experimental design. KT, JAH, TK, CC, AN, and HS helped to analyze the data. TS contributed analysis of data. YN conceived of the project, designed the experiments, and analyzed the data. All authors read and approved the final manuscript.

Acknowledgements
We thank K Kubota for her secretarial assistance, and T Sugimoto, K Shiozaki, T Enya and Y Namura for their technical assistance. We also thank Dr. Somasekhar Bhamidipati (Rigel Inc.) for the synthesis of R723. This study was financially supported in part by an Inochi-no-Iro ALS Research Grant and a Grant-in-Aid for Young Scientists (B) to ST (Number 24790883) from the Japanese Ministry of Education, Culture, Sports, Science and Technology (MEXT); a Grant-in-Aid for Scientific Research (GSR, S) to HK (Number 20229007) from MEXT; a GSR on Innovative Areas to HM (Number 24111531) from MEXT; a Health Labour Sciences Research Grant to TO from the Japanese Ministry of Health, Labour and Welfare; and a Health Labour Sciences Research Grant for Intractable Diseases to YN (Number 22590931) from the Japanese Ministry of Health, Labour and Welfare. The funders had no role in study design, data collection and analysis, decision to publish, or preparation of the manuscript.

Author details
[1]Department of Neurology, Osaka University Graduate School of Medicine, 2-2 Yamadaoka, Suita, Osaka 565-0871, Japan. [2]Department of Molecular Immunology, Research Institute for Microbial Disease, WPI Immunology Frontier Research Center (IFReC), Osaka University, 3-1 Yamadaoka, Suita, Osaka 565-0871, Japan. [3]Rigel Pharmaceuticals, Inc., 1180 Veterans Blvd., South San Francisco, CA 94080, USA. [4]Department of Mathematical Sciences, Hirosaki University Graduate School of Science and Technology, 3 Bunkyo-cho, Hirosaki, Aomori 036-8561, Japan. [5]Department of Neurology, National Hospital Organization Toneyama National Hospital, 5-1-1 Toneyama, Toyonaka, Osaka 560-0045, Japan.

Received: 28 May 2014 Accepted: 6 October 2014
Published online: 19 October 2014

References

1. Tada S, Okuno T, Yasui T, Nakatsuji Y, Sugimoto T, Kikutani H, Sakoda S: **Deleterious effects of lymphocytes at the early stage of neurodegeneration in an animal model of amyotrophic lateral sclerosis.** *J Neuroinflammation* 2011, **8**:19.
2. Tada S, Yasui T, Nakatsuji Y, Okuno T, Koda T, Mochizuki H, Sakoda S, Kikutani H: **BAFF controls neural cell survival through BAFF receptor.** *PLoS One* 2013, **8**:e70924.
3. Zhao W, Beers DR, Appel SH: **Immune-mediated mechanisms in the pathoprogression of amyotrophic lateral sclerosis.** *J Neuroimmune Pharmacol* 2013, **8**:888–899.
4. Aebischer J, Cassina P, Otsmane B, Moumen A, Seilhean D, Meininger V, Barbeito L, Pettmann B, Raoul C: **IFNgamma triggers a LIGHT-dependent selective death of motoneurons contributing to the non-cell-autonomous effects of mutant SOD1.** *Cell Death Differ* 2011, **18**:754–768.
5. Okuno T, Nakatsuji Y, Kumanogoh A, Koguchi K, Moriya M, Fujimura H, Kikutani H, Sakoda S: **Induction of cyclooxygenase-2 in reactive glial cells by the CD40 pathway: relevance to amyotrophic lateral sclerosis.** *J Neurochem* 2004, **91**:404–412.
6. Butovsky O, Siddiqui S, Gabriely G, Lanser AJ, Dake B, Murugaiyan G, Doykan CE, Wu PM, Gali RR, Iyer LK, Lawson R, Berry J, Krichevsky AM, Cudkowicz ME, Weiner HL: **Modulating inflammatory monocytes with a unique microRNA gene signature ameliorates murine ALS.** *J Clin Invest* 2012, **122**:3063–3087.
7. Vakil E, Tefferi A: **BCR-ABL1-negative myeloproliferative neoplasms: a review of molecular biology, diagnosis, and treatment.** *Clin Lymphoma Myeloma Leuk* 2011, **11**(Suppl 1):S37–S45.
8. Kiu H, Nicholson SE: **Biology and significance of the JAK/STAT signalling pathways.** *Growth Factors* 2012, **30**:88–106.
9. Seavey MM, Dobrzanski P: **The many faces of Janus kinase.** *Biochem Pharmacol* 2012, **83**:1136–1145.
10. Liu Y, Holdbrooks AT, De Sarno P, Rowse AL, Yanagisawa LL, McFarland BC, Harrington LE, Raman C, Sabbaj S, Benveniste EN, Qin H: **Therapeutic efficacy of suppressing the Jak/STAT pathway in multiple models of experimental autoimmune encephalomyelitis.** *J Immunol* 2014, **192**:59–72.
11. Stump KL, Lu LD, Dobrzanski P, Serdikoff C, Gingrich DE, Dugan BJ, Angeles TS, Albom MS, Ator MA, Dorsey BD, Ruggeri BA, Seavey MM: **A highly selective, orally active inhibitor of Janus kinase 2, CEP-33779, ablates disease in two mouse models of rheumatoid arthritis.** *Arthritis Res Ther* 2011, **13**:R68.
12. Taylor P, Genovese M, Keystone E, Schlichting D, Beattie S, Macias W: **A1.72 Baricitinib, an oral janus kinase inhibitor, in the treatment of rheumatoid arthritis: safety and efficacy in an open-label, long-term extension study[1].** *Ann Rheum Dis* 2014, **73**(1):A31.
13. Sandborn WJ, Ghosh S, Panes J, Vranic I, Wang W, Niezychowski W, Study AI: **A phase 2 study of tofacitinib, an oral Janus kinase inhibitor, in patients with Crohn's disease.** *Clin Gastroenterol Hepatol* 2014, **12**:1485–1493.
14. Ports WC, Khan S, Lan S, Lamba M, Bolduc C, Bissonnette R, Papp K: **A randomized phase 2a efficacy and safety trial of the topical Janus kinase inhibitor tofacitinib in the treatment of chronic plaque psoriasis.** *Br J Dermatol* 2013, **169**:137–145.
15. Shide K, Kameda T, Markovtsov V, Shimoda HK, Tonkin E, Fang S, Liu C, Gelman M, Lang W, Romero J, McLaughlin J, Bhamidipati S, Clough J, Low C, Reitsma A, Siu S, Pine P, Park G, Torneros A, Duan M, Singh R, Payan DG, Matsunaga T, Hitoshi Y, Shimoda K: **R723, a selective JAK2 inhibitor, effectively treats JAK2V617F-induced murine myeloproliferative neoplasm.** *Blood* 2011, **117**:6866–6875.
16. Beers DR, Zhao W, Liao B, Kano O, Wang J, Huang A, Appel SH, Henkel JS: **Neuroinflammation modulates distinct regional and temporal clinical responses in ALS mice.** *Brain Behav Immun* 2011, **25**:1025–1035.
17. Reichel A: **The role of blood-brain barrier studies in the pharmaceutical industry.** *Curr Drug Metab* 2006, **7**:183–203.
18. Bhattacharjee A, Shukla M, Yakubenko VP, Mulya A, Kundu S, Cathcart MK: **IL-4 and IL-13 employ discrete signaling pathways for target gene expression in alternatively activated monocytes/macrophages.** *Free Radic Biol Med* 2013, **54**:1–16.
19. Zhao J, Li G, Zhang Y, Su X, Hang C: **The potential role of JAK2/STAT3 pathway on the anti-apoptotic effect of recombinant human erythropoietin (rhEPO) after experimental traumatic brain injury of rats.** *Cytokine* 2011, **56**:343–350.

doi:10.1186/s12974-014-0179-2
Cite this article as: Tada *et al.*: Partial suppression of M1 microglia by Janus kinase 2 inhibitor does not protect against neurodegeneration in animal models of amyotrophic lateral sclerosis. *Journal of Neuroinflammation* 2014 **11**:179.

Glycobiology vol. 24 no. 5 pp. 469–475, 2014
doi:10.1093/glycob/cwu014
Advance Access publication on February 28, 2014

Chondroitin 6-*O*-sulfate ameliorates experimental autoimmune encephalomyelitis

Katsuichi Miyamoto[1,2], Noriko Tanaka[2], Kota Moriguchi[3], Rino Ueno[2], Kenji Kadomatsu[4], Hiroshi Kitagawa[5], and Susumu Kusunoki[2]

[2]Department of Neurology, Kinki University School of Medicine, Osaka-Sayama, Japan; [3]Division of Neurology, Department of Internal Medicine 3, National Defense Medical College, Tokorozawa, Japan; [4]Department of Biochemistry, Nagoya University School of Medicine, Nagoya, Japan; and [5]Department of Biochemistry, Kobe Pharmaceutical University, Kobe, Japan

Received on August 19, 2013; revised on February 20, 2014; accepted on February 21, 2014

Chondroitin sulfate proteoglycans (CSPGs) are the main component of the extracellular matrix in the central nervous system (CNS) and influence neuroplasticity. Although CSPG is considered an inhibitory factor for nerve repair in spinal cord injury, it is unclear whether CSPG influences the pathogenetic mechanisms of neuroimmunological diseases. We induced experimental autoimmune encephalomyelitis (EAE) in chondroitin 6-*O*-sulfate transferase 1-deficient (C6st1$^{-/-}$) mice. C6ST1 is the enzyme that transfers sulfate residues to position 6 of *N*-acetylgalactosamine in the sugar chain of CSPG. The phenotypes of EAE in C6st1$^{-/-}$ mice were more severe than those in wild-type (WT) mice were. In adoptive-transfer EAE, in which antigen-reactive T cells from WT mice were transferred to C6st1$^{-/-}$ and WT mice, phenotypes were significantly more severe in C6st1$^{-/-}$ than in WT mice. The recall response of antigen-reactive T cells was not significantly different among the groups. Furthermore, the number of pathogenic T cells within the CNS was also not considerably different. When EAE was induced in C6ST1 transgenic mice with C6ST1 overexpression, the mice showed considerably milder symptoms compared with those in WT mice. In conclusion, the presence of sulfate at position 6 of *N*-acetylgalactosamine of CSPG may influence the effecter phase of EAE to prevent the progression of pathogenesis. Thus, modification of the carbohydrate residue of CSPG may be a novel therapeutic strategy for neuroimmunological diseases such as multiple sclerosis.

Keywords: central nervous system / chondroitin sulfate / experimental autoimmune encephalomyelitis / multiple sclerosis / myelin oligodendrocyte glycoprotein / proteoglycan

[1]To whom correspondence should be addressed: Tel: +81-723-66-0221; Fax: +81-723-68-4846; e-mail: miyamoto@med.kindai.ac.jp

Introduction

Chondroitin sulfate proteoglycans (CSPGs) are a family of glycosaminoglycans consisting of glucuronic acid, *N*-acetylgalactosamine and sulfate. CSPG is the main constituent of the extracellular matrix in the central nervous system (CNS) and influences neuroplasticity (Rolls et al. 2006). For example, CSPG levels are up-regulated after CNS injury (McKeon et al. 1999; Asher et al. 2001; Jones et al. 2002) and during the course of chronic neurodegenerative disorders such as multiple sclerosis (Sobel and Ahmed 2001) and Alzheimer's disease (Inoue 2001). CSPG attenuates regeneration in the CNS (Properzi et al. 2003; Silver and Miller 2004) by inhibiting neuronal growth (Bradbury et al. 2002; Grimpe and Silver 2002) and regulating the activation of immune components (Fitch and Silver 1997).

For instance, CSPG inhibits axonal regeneration in spinal cord injury models and, conversely, CSPG degradation by the enzyme chondroitinase ABC promotes repair (Bradbury et al. 2002; Chau et al. 2004; Huang et al. 2006). In general, inhibition of non-systemic neuronal projection protects the neuronal network. These reports suggest that CS moieties of CSPGs are responsible for PNN formation and control of the critical period plasticity. However, importance of sulfation pattern of CS chains in the plasticity has been overlooked in these previous studies due to the exclusive use of ChABC that degrades all CS chains, irrespective of their sulfation status. Sulfation profiles of CS chains change dramatically during brain development (Mikami and Kitagawa 2013). Although the role of CSPG in autoimmune disease has not been analyzed in detail, some reports have indicated that CSPG promotes recovery in CNS immunopathologies such as experimental autoimmune encephalomyelitis (EAE). For example, administration of CSPG alleviates the clinical symptoms of EAE and reduces microglia activation and the number of infiltrating T cells (Zhou et al. 2010). Furthermore, the deletion of protein tyrosine phosphatase receptor type Z as CSPG in the CNS delays recovery from paralysis associated with EAE. These results indicate that CSPG has a role in CNS recovery and might therefore be helpful in overcoming inflammation-induced neurodegenerative conditions (Harroch et al. 2002).

Chondroitin 6-sulfotransferase (C6ST) catalyzes the transfer of sulfate to position 6 of the *N*-acetylgalactosamine residue of chondroitin. Sulfation that occurs mainly at the C-6 position of the internal GalNAc residue produces chondroitin 6-sulfate (C6S), whereas the C-4 sulfated form is called (C4S).

C6S is the dominant form of chondroitin in the fetal period; however, the percentage of chondroitin 4-sulfate increases

during development. Sulfation patterns vary depending on organ, age, cell progression and other factors. For instance, distinctive increases in C6S are seen in the spleen, lung, bone marrow and eye, and C6S plays a role in the maintenance of naive T lymphocytes in the spleen of young mice (Uchimura et al. 2002). Molecular cloning of human C6ST has revealed two orthologous genes, *C6ST1* (Fukuta et al. 1998; Uchimura et al. 1998) and *C6ST2* (Kitagawa et al. 2000). Expression of both isoforms in the brain is evident during development but negligible in adulthood. C6ST1 is one of the sulfotransferases involved in the biosynthesis of sulfated glycosaminoglycans; however, in vivo functional analysis of C6ST1-deficient mice shows no apparent abnormality in brain development (Uchimura et al. 2002). In the present study, we analyzed the role of CSPG in EAE using C6ST1-deficient mice.

Materials and methods

Mice

Wild-type (WT) C57BL/6 mice were purchased from Clea Japan (Tokyo, Japan). C6ST1$^{-/-}$ mice were originally obtained from Dr. Kadomatsu (Nagoya, Japan) and have been described previously. The mice had been backcrossed to the C57BL/6 background for more than five generations.

Mice were rendered deficient in the *C6st1*$^{-/-}$ gene via embryonic stem cell technology. C6st1$^{-/-}$ mice were born at approximately the expected frequency and were viable through adulthood. Brain development was normal in C6st1$^{-/-}$ mice. Further analysis revealed that the number of CD62L^{+}CD44^{low} T lymphocytes corresponding to naive T lymphocytes in the spleen of C6st1$^{-/-}$ mice was significantly decreased, whereas that in other secondary lymphoid organs was unchanged (Uchimura et al. 2002). Genotyping of C6ST1$^{-/-}$ mice was performed with polymerase chain reaction as described elsewhere.

C6ST1 transgenic mice (C6ST1^{tg}) were obtained from Dr. Kitagawa (Miyata et al. 2012). Full-length human C6ST1 complementary DNA was amplified with reverse transcription polymerase chain reaction using a human placenta complementary DNA library and cloned into the EcoRI site of a pCAG vector, which drives transgene expression using a chicken β-actin promoter and cytomegalovirus enhancer (Niwa et al. 1991). Plasmid DNA was injected into C57BL6 embryos, which were placed into pseudopregnant females to produce transgenic offspring. Transgenic mice were identified with Southern blot using tail DNA and were mated with C57BL6 WT mice. Mice were kept under specific pathogen-free conditions in an environmentally controlled, clean room. All experiments were conducted according to institutional ethics guidelines for animal experiments and safety guidelines for gene manipulation experiments. These mice were maintained under specific pathogen-free conditions. All mice for experiments were 8–12 weeks old.

Peptides

Myelin oligodendrocyte glycoprotein (MOG_{35-55}) (single-letter amino acid code, MEVGWYRSPFSRVVHLYRNGK) was synthesized by Tore Research Institute (Tokyo, Japan). The peptides were of >90% purity, as determined by high-performance liquid chromatography (HPLC).

Induction and assessment of EAE

Mice were injected subcutaneously in both flanks with 200 μL of inoculum containing 100 μg MOG_{35-55} and 0.5 mg *Mycobacterium tuberculosis* H37Ra (Difco Laboratories, Detroit, MI) in incomplete Freund's adjuvant. Pertussis toxin (200 ng; List Biological Laboratories Inc., Campbell, CA) was injected intravenously on days 0 and 2 after immunization. For EAE induction in the adoptive-transfer model, recipient mice were injected intravenously with encephalitogenic cells (prepared as in Preparation of cells for EAE induction in the adoptive-transfer model section) and 200 ng of pertussis toxin. Immunized mice were examined daily and scored as follows: 0, no clinical signs; 1, limp tail; 2, partial hind leg paralysis; 3, total hind leg or partial hind and front leg paralysis; 4, total hind leg and partial front leg paralysis; 5, moribund or dead. Mice were examined daily in a blind fashion for signs of EAE.

Preparation of cells for EAE induction in the adoptive-transfer model

For preparation of MOG-specific cells to induce EAE in the adoptive-transfer model, mice were immunized with MOG/complete Freund's adjuvant following the protocol used to induce EAE. Draining lymph nodes (LNs) were collected 10 days later, and a single-cell suspension was prepared. The cells were stimulated with 30 μg/mL MOG_{35-55} in 24-well flat-bottomed plates (5×10^6 cells/well) in T-cell medium (RPMI media enriched with 10% fetal bovine serum, 2 mM L-glutamine, 5×10^{-5} M 2-ME, nonessential amino acids, sodium pyruvate and penicillin/streptomycin). Recombinant mouse interleukin (IL)-12 was added at 20 ng/mL. Four days after initiation of the cultures, cells were harvested, and CD4^{+} cells were selected using a column (R&D, Minneapolis, MN). Ten million CD4^{+} cells were injected intravenously into recipient mice as described above for EAE induction.

Establishment of a MOG_{35-55}-specific T-cell line

A MOG-specific T-cell line was established using cells for adoptive-transfer EAE as described above. The cells were cultured in T-cell medium with 10 ng/mL of IL-2. Half of the medium was replaced every few days. Stimulation with 30 μg/mL MOG_{35-55} was performed every 10 days with irradiated (30 Gy) splenocytes as antigen-presenting cells.

MOG_{35-55}-specific T-cell proliferation assay

For proliferation assays, mice were immunized with peptide/CFA as described above, but the mice were not treated with pertussis toxin. A single-cell suspension was prepared from the draining LNs 10 days after immunization. Cells were cultured in Dulbecco's modified Eagle medium (Gibco, Grand Islands, NY) supplemented with 5×10^{-5} M 2-mercaptoethanol, 2 mM L-glutamine, 100 U/mL of penicillin and streptomycin and 1% autologous mouse serum and seeded onto 96-well flat-bottomed plates (1×10^6 cells/well). The cells were restimulated with peptide for 72 h at 37°C in humidified air with 5% CO_2. To measure cellular proliferation, [^{3}H]-thymidine was added (1 mCi/well) and uptake of the radioisotope during the final 18 h of culture was counted with a beta-1205 counter (Pharmacia, Uppsala, Sweden). To evaluate the proliferative

responses of LN cells to the peptide, we determined the delta (Δ)c.p.m. value for cells in each well by subtracting the background c.p.m. and then used the mean of these values to represent each mouse.

Detection of cytokines

In parallel, LN cells from immunized mice were cultured with peptide concentrations of 0, 1, 10 and 100 μg/mL. Supernatants from the cultures were harvested 48 h postactivation and tested for the presence of various cytokines. The concentrations of interferon gamma (IFN-g), IL-2, IL-4 and IL-10 in the supernatants were measured with sandwich enzyme-linked immunosorbent assay according to the manufacturer guideline (BD Biosciences, San Jose, CA). Limits of detection for IFN-g, IL-2, IL-4 and IL-10 were 195, 25, 12.5, and 50 pg/mL, respectively.

Analysis of infiltrating cells isolated from the CNS

Wt and C6ST1$^{-/-}$ mice were anesthetized with diethyl ether on day 9 after EAE induction. After perfusion with phosphate-buffered saline, the brain and spinal cord were removed and homogenized. After washing with phosphate-buffered saline, mononuclear cells were isolated using Percoll gradient (Amersham Biosciences, Piscataway, NJ) and counted (Miyamoto et al. 2006). The cells were stained with phycoerythrin-labeled anti-CD4 antibody (BD Biosciences) and analyzed with flow cytometry using a BD FACSCalibur device. As a control, naive mice were also analyzed for the infiltration of cells into the CNS using the same method.

Pathological analysis

The brain and spinal cord were removed on day 14 after the induction of EAE. Ten-micrometer-thick frozen sections were fixed with acetone and stained with hematoxylin and eosin or Luxol fast blue.

HPLC analysis

Soluble CSPG fractions from brain were prepared as described previously (Kitagawa et al. 1997). In brief, brains from WT or C6st1$^{-/-}$ mice, at pre- or postimmunization EAE, were homogenized in ice-cold PBS containing EDTA and phenylmethylsulfonyl fluoride. After centrifugation, supernatant fluids were concentrated, and then washed with Tris–HCl buffer containing sodium acetate. The protein concentration of the proteoglycan fractions was determined using the BCA protein assay kit. These fractions were first digested using chondroitin ABC lyase and evaporated to dryness.

The digests were derivatized with 2-aminobenzamide according to the manufacturer's instructions (SIGNAL™ labeling kit, Oxford GlycoSystems). The labeled disaccharides were analyzed by on an amine-bound silica PA03 column. The HPLC was performed in an LC-10AS system (Shimadzu Co., Kyoto, Japan).

Statistics

Non-parametric Mann–Whitney *U* tests were used to calculate significant levels for all measurements. Values of $P < 0.05$ were considered statistically significant.

Results

Exacerbation of EAE in C6ST1$^{-/-}$ mice

To examine the role of C6ST1 in the development of EAE, we first performed active immunization to establish EAE. The clinical symptoms of EAE in C6ST1$^{-/-}$ mice were more severe than those in WT mice were. Statistically, a significant difference in EAE maximum score and cumulative score was found between C6ST1$^{-/-}$ and WT mice (Figure 1, Table I). Histological comparison of the thoracic regions of the spinal cord demonstrated exacerbated monocyte infiltration and demyelination in C6ST1$^{-/-}$ mice compared with WT mice (not shown). We next performed adoptive-transfer EAE. When we transferred MOG-reactive T cells from WT mice to C6ST1$^{-/-}$ or WT mice, the severity of EAE in the C6ST1$^{-/-}$ mice was significantly higher than that in WT mice (Figure 2; Table I). These results indicate that a lack of C6S does not affect the induction phase of EAE but exhibits effects during the effector phase of EAE.

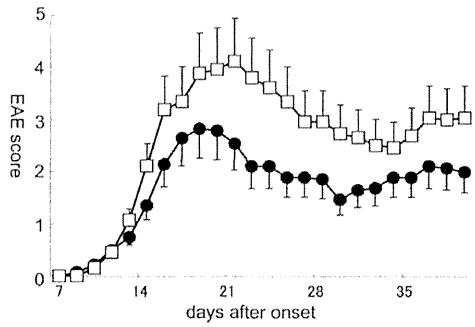

Fig. 1. Exacerbation of experimental autoimmune encephalomyelitis (EAE) in C6ST1$^{-/-}$ mice. EAE was induced in C6ST1$^{-/-}$ (open squares) or WT (closed circles) mice via immunization with myelinoligodendrocyte glycoprotein (MOG_{35-55}) in complete Freund's adjuvant (CFA) as described in Materials and methods section. Statistical analysis is shown in Table IA. Two independent experiments are expressed as the mean EAE score.

Table I. Statistical analysis of clinical EAE scores

Mouse	Incidence	Max score	Cumulative score
A			
C6ST1$^{-/-}$	24/26 (92.3%)	3.08 ± 0.25*	30.6 ± 3.4*
WT	20/28 (71.4%)	2.25 ± 0.32	20.2 ± 3.3
Recipient mouse	Incidence	Max score	Cumulative score
B			
C6ST1$^{-/-}$	8/10 (80.0%)	2.15 ± 0.48	13.4 ± 3.4*
WT	6/11 (54.5%)	1.00 ± 0.33	4.0 ± 1.7

(A) Active-immunization EAE. Each mouse was immunized with MOG_{35-55} peptide for the induction of EAE. The data are the same as in Figure 1.
(B) Adoptive-transfer EAE. One million encephalitogenic $CD4^+$ T cells from WT mice were injected intravenously into WT or C6ST1$^{-/-}$ mice (recipient). The data are the same as in Figure 4.
Mean ± SEM of the following parameters is shown: maximum score of EAE (max score), incidence of paralyzed mice among sensitized rats (Incidence), summation of the clinical scores from days 0 to 35 (Cumulative score). The statistical significance of the difference was determined using ANOVA, *$P < 0.05$ vs. WT mice.

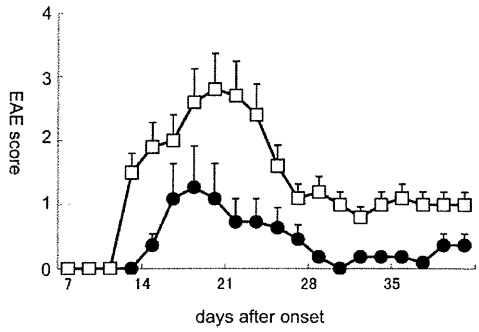

Fig. 2. Chondroitin 6-sulfotransferase plays a role in the effector phase of EAE. Encephalitogenic T cells were prepared by immunizing WT mice and culturing their LN cells in the presence of MOG and interleukin-12 for 4 days. One million $CD4^+$ cells were injected into the tail vein of WT (closed circles) or $C6ST1^{-/-}$ mice (open squares). EAE clinical scores were assessed as described in Table IB. These data are shown as mean clinical scores ± standard error of the mean (SEM).

Spinal cord from $C6ST1^{-/-}$ mice shows severe cell infiltration in comparison with it from WT (Figure 3). This shows that the presence of C6ST inhibits the infiltration of pathogenic lymphocyte in EAE.

C6ST1 has no effect on the recall response of MOG-specific T cells

To determine the mechanisms of C6S in T-cell activation, we examined the proliferative response and cytokine production of draining LN cells in vitro. $C6ST1^{-/-}$ or WT mice were immunized with MOG_{35-55}. Ten days after immunization, draining LN cells were collected and cultured with MOG_{35-55} peptide. As shown in Figure 4, no significant difference was found in the proliferative responses of MOG-reactive T cells in $C6ST1^{-/-}$ and WT mice. We next examined the levels of cytokines in the culture supernatant using enzyme-linked immunosorbent assay. Levels of IFN-g, IL-4, IL-10 and IL-17 in the culture supernatants of LN cells obtained from $C6ST1^{-/-}$ and WT mice were similar (data not shown).

Lack of C6S has no effect on the infiltration of pathogenic T cells into the CNS

To analyze the mechanism of C6S on the infiltration of the inflammatory cells into the CNS, we isolated mononuclear cells in CNS samples obtained from each mouse on day 9 of active-immunization EAE. This period occurs just before the onset of EAE in WT mice; none of the mice exhibited EAE symptoms at that time. As shown in Figure 5, the $CD4^+$ cell number in the CNS samples from $C6ST1^{-/-}$ mice was not significantly different from that in the samples from WT mice (14.3 ± 2.8 vs. 13.3 ± 2.6, as mean ± standard error of the mean, $\times 10^5$). This result suggests that C6S has no effect on the migration of pathogenic T cells into the CNS.

Expression level of C6S in CNS during EAE

To confirm whether C6S is up-regulated in CNS, HPLC analysis was performed. Figure 6 shows that C-unit CS (C6S) did not detected in brains from $C6st1^{-/-}$ mice. In WT mice, increased expression of C-unit CS did not observed in brains from EAE immunized mice in comparison with brains from naive mice.

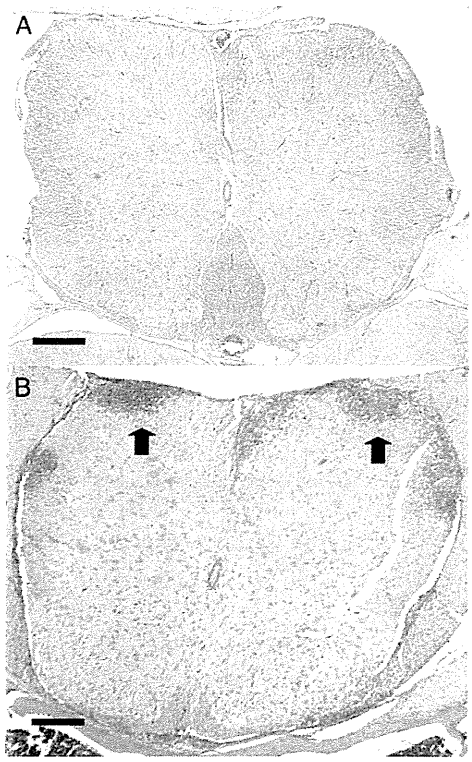

Fig. 3. Histopathological findings of spinal cord. Spinal cord from $C6ST1^{-/-}$ mice (**B**) shows severe cell infiltration (arrow) in comparison with it from WT (**A**).

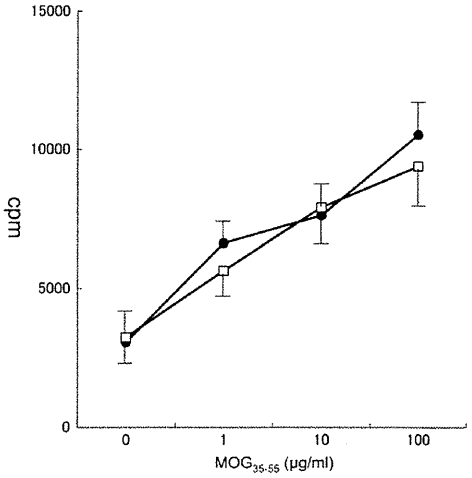

Fig. 4. Comparison of MOG_{35-55}-specific T-cell response in $C6ST1^{-/-}$ and WT mice. Popliteal and inguinal LN cells from $C6ST1^{-/-}$ (open squares) or WT (closed circles) mice were incubated in the presence of MOG_{35-55} for 48 h. Proliferative response was determined by the uptake of $[^3H]$ thymidine. Representative data of two independent experiments are shown ($n = 12$ for each group). Error bars represent SEM.

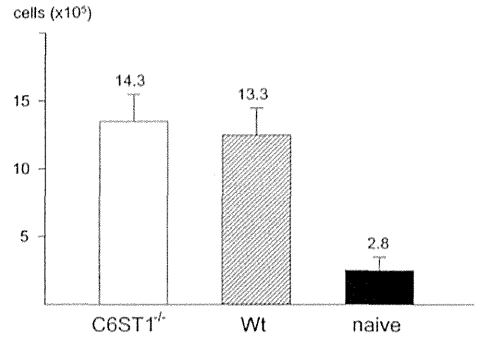

Fig. 5. Analysis of infiltrating cells isolated from the CNS. Infiltrating cells in the CNS from each mouse were collected as described in Materials and methods section. The infiltrating $CD4^+$ T cells were analyzed with flow cytometry. The data are presented as mean ± SEM ($\times 10^5$), WT (13.3 ± 2.6, $n = 3$), *C6ST1*$^{-/-}$ (14.3 ± 2.8, $n = 3$) and naive mice (1.4 ± 0.3, $n = 3$). $^*P < 0.05$ by Mann–Whitney *U* test.

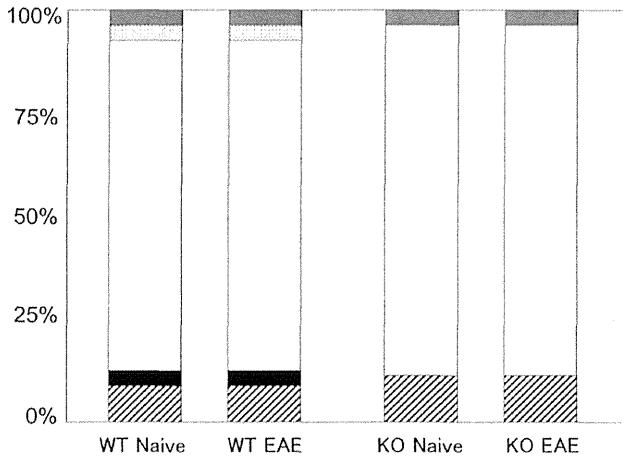

Fig. 6. C6S is not up-regulated during the development EAE. To confirm whether C-unit CS (C6S, closed square) is up-regulated in the CNS during the development EAE, HPLC analysis was performed. The fractionation and analysis of oligosaccharides were carried out by HPLC as described in Materials and methods section. This shows that the expression level of C6S is no change during the development EAE.

Amelioration of EAE in C6ST1^{tg} *mice*

Next, we analyzed whether overexpression of C6ST reduces the progression of EAE. EAE was induced in C6ST1^{tg} mice overexpressing C6ST1. The maximum score of C6ST1^{tg} mice was significantly lower than that of WT mice. The cumulative score of C6ST1^{tg} mice was also significantly lower than that of WT mice. In contrast, the score of C6ST1$^{-/-}$ mice was significantly higher than that of WT mice (Figure 7; Table II). These results suggested that C6ST1 ameliorates the pathogenesis of EAE.

Discussion

We have previously shown that the onset of EAE is delayed in mice lacking complex gangliosides owing to the lack of

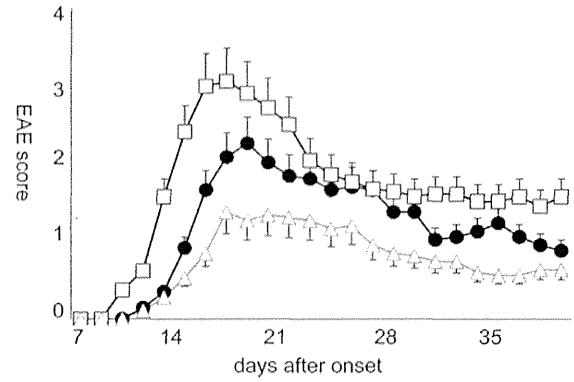

Fig. 7. Overexpression of chondroitin 6-sulfotransferase ameliorates EAE. EAE was induced in C6ST1$^{-/-}$ (open squares), C6ST1^{tg} (open triangle) or WT (closed circles) mice via immunization with MOG_{35-55} in CFA as described in Materials and methods section. Statistical analysis is shown in Table II. Two independent experiments are shown as the mean clinical score ± SEM.

Table II. Statistical analysis of clinical EAE scores

Mouse	Incidence	Max score	Cumulative score
C6ST1$^{-/-}$	15/16 (93.8%)	3.66 ± 0.28*	41.0 ± 4.1*
C6ST1-Tg	11/14 (78.6%)	1.96 ± 0.36*#	18.0 ± 4.5#
WT	12/14 (85.7%)	3.00 ± 0.38	28.5 ± 4.6

Active-immunization EAE. Each mouse was immunized with MOG_{35-55} peptide for the induction of EAE. The data are the same as in Figure 7. Mean ± SEM of the following parameters is shown: maximum score of EAE (max score), incidence of paralyzed mice among sensitized rats (incidence), summation of the clinical scores from days 0 to 35 (cumulative score). The statistical significance of the difference was determined using ANOVA, $^*P < 0.05$ vs. WT mice, $^{\#}P < 0.001$ vs. C6ST1$^{-/-}$ mice.

GM2/GD2 synthase. The carbohydrate portion of complex gangliosides may be involved in the migration of activated T lymphocytes across the blood–brain barrier (Miyamoto et al. 2008). Thus, modification of the carbohydrate portion of the glycoconjugates may affect the pathogenetic mechanisms of EAE. In the current study, we demonstrated that CSPG is involved in the pathogenesis of EAE. Active-immunization and adoptive-transfer experiments showed that lack of C6ST1 exacerbated the disease severity of EAE in the effector phase. No difference was found in the recall response of lymphocytes to MOG_{35-55} in C6ST1-deficient mice compared with WT mice. Furthermore, the lack of C6ST1 did not affect the passage of activated T lymphocytes across the blood–brain barrier in EAE. Moreover, overexpression of C6ST reduced the pathogenesis of EAE. The results suggest that C6S could have a neuroprotective effect in the effector phase of EAE. Because C-unit CS (C6S) does not increase during EAE, C6S may be acting protectively regardless of the immunization.

Recently, CSPG has been implicated in several intriguing biological phenomena, such as the regulation of growth factor functions (Deepa et al. 2002), cell division (Sugahara and Mikami 2007) and neuritogenesis (Li et al. 2007). In addition, a missense mutation of C6ST1 has been demonstrated to

abolish C6ST activity almost completely and cause severe human chondrodysplasia with major involvement of the spine (Thiele et al. 2004; van Roij et al. 2008).

In a spinal cord injury model, CSPG inhibits re-innervation, and a CSPG-degrading enzyme promotes axonal regeneration (Kawano et al. 2005). Chondroitinase ABC treatment up-regulates regeneration-associated proteins in injured neurons and promotes the regeneration of both ascending sensory projections and descending corticospinal tract axons (Bradbury et al. 2002). Treatment with transforming growth factor-beta1 upregulates keratan sulfate and CSPG biosynthesis (Yin et al. 2009), and it promotes the expression of C6ST1 (Properzi et al. 2005) in microglia after brain injury. CSPG3, or neurocan, is up-regulated in the periventricular white matter and cortex in the effector phase of EAE. CSPG3 is indicative of cell recruitment for repair processes and is confirmed by the presence of thin myelin sheaths in the plaques (Sajad et al. 2011). Thus, CSPG3 may play a crucial role in CNS regeneration in EAE.

Phosphacan is a CSPG that accelerates nerve recovery and has crucial roles in the maintenance of oligodendrocytes (Ranjan and Hudson. 1996). Studies have shown that the administration of CSPG causes severe clinical symptoms in EAE (Rolls et al. 2006). Zhou et al. demonstrates that a disaccharide fraction of 6-sulfated C units reduces EAE, while 4-sulfated CS-A may actually make things worse (Zhou et al. 2010). The variable results of these experiments indicate that a consensus has not yet been reached on the therapeutic effect of CSPG. In our study, C6S displayed a neuroprotective effect in EAE. Modification of sulfation pattern to increase C6S levels in the CNS is used as a treatment for EAE. C6S may inhibit the spread of pathogenic T cells in the CNS. Although CSPG prevents nerve regeneration in the recovery phase of the nerve injury model, CSPG may prevent disease progression in the acute phase of EAE. Thus, modification of the carbohydrate structure of CSPG could be used as a new therapeutic method for neuroimmunological diseases such as multiple sclerosis.

Funding

This work was supported in part by Health Sciences Research Grants (Comprehensive Research on Disability Health and Welfare and Research on Intractable Diseases [H23-017]) from the Ministry of Health, Labour and Welfare of Japan and a Grant-in-Aid for Scientific Research (24110518) from the Ministry of Education, Culture, Sports, Science and Technology of Japan.

Conflict of interest

None declared.

Abbreviations

C6ST, chondroitin 6-sulfotransferase; CSPG, chondroitin sulfate proteoglycan; CNS, central nervous system; EAE, experimental autoimmune encephalomyelitis; HPLC, high-performance liquid chromatography; LN, lymph node; MOG, myelin oligodendrocyte glycoprotein

References

Asher RA, Morgenstern DA, Moon LD, Fawcett JW. 2001. Chondroitin sulphate proteoglycans: Inhibitory components of the glial scar. *Prog Brain Res.* 132:611–619.

Bradbury EJ, Moon LD, Popat RJ, King VR, Bennett GS, Patel PN, Fawcett JW, McMahon SB. 2002. Chondroitinase ABC promotes functional recovery after spinal cord injury. *Nature.* 416:636–640.

Chau CH, Shum DK, Li H, Pei J, Lui YY, Wirthlin L, Chan YS, Xu XM. 2004. Chondroitinase ABC enhances axonal regrowth through Schwann cell-seeded guidance channels after spinal cord injury. *FASEB J.* 18:194–196.

Deepa SS, Umehara Y, Higashiyama S, Itoh N, Sugahara K. 2002. Specific molecular interactions of oversulfated chondroitin sulfate E with various heparin-binding growth factors. Implications as a physiological binding partner in the brain and other tissues. *J Biol Chem.* 277:43707–43716.

Fitch MT, Silver J. 1997. Activated macrophages and the blood-brain barrier: Inflammation after CNS injury leads to increases in putative inhibitory molecules. *Exp Neurol.* 148:587–603.

Fukuta M, Kobayashi Y, Uchimura K, Kimata K, Habuchi O. 1998. Molecular cloning and expression of human chondroitin 6-sulfotransferase. *Biochim Biophys Acta.* 1399:57–61.

Grimpe B, Silver J. 2002. The extracellular matrix in axon regeneration. *Prog Brain Res.* 137:333–349.

Harroch S, Furtado GC, Brueck W, Rosenbluth J, Lafaille J, Chao M, Buxbaum JD, Schlessinger J. 2002. A critical role for the protein tyrosine phosphatase receptor type Z in functional recovery from demyelinating lesions. *Nat Genet.* 32:411–414.

Huang WC, Kuo WC, Cherng JH, Hsu SH, Chen PR, Huang SH, Huang MC, Liu JC, Cheng H. 2006. Chondroitinase ABC promotes axonal re-growth and behavior recovery in spinal cord injury. *Biochem Biophys Res Commun.* 349:963–968.

Inoue S. 2001. Basement membrane and beta amyloid fibrillogenesis in Alzheimer's disease. *Int Rev Cytol.* 210:121–161.

Jones LL, Yamaguchi Y, Stallcup WB, Tuszynski MH. 2002. NG2 is a major chondroitin sulfate proteoglycan produced after spinal cord injury and is expressed by macrophages and oligodendrocyte progenitors. *J Neurosci.* 22:2792–2803.

Kawano H, Li HP, Sango K, Kawamura K, Raisman G. 2005. Inhibition of collagen synthesis overrides the age-related failure of regeneration of nigrostriatal dopaminergic axons. *J Neurosci Res.* 80:191–202.

Kitagawa H, Fujita M, Ito N, Sugahara K. 2000. Molecular cloning and expression of a novel chondroitin 6-O-sulfotransferase. *J Biol Chem.* 275:21075–21080.

Kitagawa H, Tsutsumi K, Tone Y, Sugahara K. 1997. Developmental regulation of the sulfation profile of chondroitin sulfate chains in the chicken embryo brain. *J Biol Chem.* 272:31377–31381.

Li F, Shetty AK, Sugahara K. 2007. Neuritogenic activity of chondroitin/dermatan sulfate hybrid chains of embryonic pig brain and their mimicry from shark liver. Involvement of the pleiotrophin and hepatocyte growth factor signaling pathways. *J Biol Chem.* 282:2956–2966.

McKeon RJ, Jurynec MJ, Buck CR. 1999. The chondroitin sulfate proteoglycans neurocan and phosphacan are expressed by reactive astrocytes in the chronic CNS glial scar. *J Neurosci.* 19:10778–10788.

Mikami T, Kitagawa H. 2013. Biosynthesis and function of chondroitin sulfate. *Biochim Biophys Acta.* 1830:4719–4733.

Miyamoto K, Miyake S, Mizuno M, Oka N, Kusunoki S, Yamamura T. 2006. Selective COX-2 inhibitor celecoxib prevents experimental autoimmune encephalomyelitis through COX-2-independent pathway. *Brain.* 129:1984–1992.

Miyamoto K, Takada K, Furukawa K, Furukawa K, Kusunoki S. 2008. Roles of complex gangliosides in the development of experimental autoimmune encephalomyelitis. *Glycobiology.* 18:408–413.

Miyata S, Komatsu Y, Yoshimura Y, Taya C, Kitagawa H. 2012. Persistent cortical plasticity by upregulation of chondroitin 6-sulfation. *Nat Neurosci.* 15:414–422.

Niwa H, Yamamura K, Miyazaki J. 1991. Efficient selection for high-expression transfectants with a novel eukaryotic vector. *Gene.* 108:193–199.

Properzi F, Asher RA, Fawcett JW. 2003. Chondroitin sulphate proteoglycans in the central nervous system: Changes and synthesis after injury. *Biochem Soc Trans.* 31:335–336.

Properzi F, Carulli D, Asher RA, Muir E, Camargo LM, van Kuppevelt TH, ten Dam GB, Furukawa Y, Mikami T, Sugahara K, et al. 2005. Chondroitin 6-sulphate synthesis is up-regulated in injured CNS, induced by injury-related cytokines and enhanced in axon-growth inhibitory glia. *Eur J Neurosci.* 21:378–390.

Ranjan M, Hudson LD. 1996. Regulation of tyrosine phosphorylation and protein tyrosine phosphatases during oligodendrocyte differentiation. *Mol Cell Neurosci.* 7:404–418.

Rolls A, Cahalon L, Bakalash S, Avidan H, Lider O, Schwartz M. 2006. A sulfated disaccharide derived from chondroitin sulfate proteoglycan protects against inflammation-associated neurodegeneration. *FASEB J.* 20:547–549.

Sajad M, Zargan J, Chawla R, Umar S, Khan HA. 2011. Upregulation of CSPG3 Accompanies Neuronal Progenitor Proliferation and Migration in EAE. *J Mol Neurosci.* 43:531–540.

Silver J, Miller J. 2004. Regeneration beyond the glial scar. *Nat Rev Neurosci.* 5:146–156.

Sobel RA, Ahmed AS. 2001. White matter extracellular matrix chondroitin sulfate/dermatan sulfate proteoglycans in multiple sclerosis. *J Neuropathol Exp Neurol.* 60:1198–1207.

Sugahara K, Mikami T. 2007. Chondroitin/dermatan sulfate in the central nervous system. *Curr Opin Struct Biol.* 17:536–545.

Thiele H, Sakano M, Kitagawa H, Sugahara K, Rajab A, Höhne W, Leschik G, Nürnberg P, Mundlos S. 2004. Loss of chondroitin 6-O-sulfotransferase-1 function results in severe human chondrodysplasia with progressive spinal involvement. *Proc Natl Acad Sci USA.* 101:10155–10160.

Uchimura K, Kadomatsu K, Fan QW, Muramatsu H, Kurosawa N, Kaname T, Yamamura K, Fukuta M, Habuchi O, Muramatsu T. 1998. Mouse chondroitin 6-sulfotransferase: Molecular cloning, characterization and chromosomal mapping. *Glycobiology.* 8:489–496.

Uchimura K, Kadomatsu K, Nishimura H, Muramatsu H, Nakamura E, Kurosawa N, Habuchi O, El-Fasakhany FM, Yoshikai Y, Muramatsu T. 2002. Functional analysis of the chondroitin 6-sulfotransferase gene in relation to lymphocyte subpopulations, brain development, and oversulfated chondroitin sulfates. *J Biol Chem.* 277:1443–1450.

van Roij MH, Mizumoto S, Yamada S, Morgan T, Tan-Sindhunata MB, Meijers-Heijboer H, Verbeke JI, Markie D, Sugahara K, Robertson SP. 2008. Spondyloepiphyseal dysplasia, Omani type: Further definition of the phenotype. *Am J Med Genet.* 146:2376–2384.

Yin J, Sakamoto K, Zhang H, Ito Z, Imagama S, Kishida S, Natori T, Sawada M, Matsuyama Y, Kadomatsu K. 2009. Transforming growth factor-beta1 upregulates keratan sulfate and chondroitin sulfate biosynthesis in microglias after brain injury. *Brain Res.* 1263:10–22.

Zhou J, Nagarkatti P, Zhong Y, Nagarkatti M. 2010. Immune modulation by chondroitin sulfate and its degraded disaccharide product in the development of an experimental model of multiple sclerosis. *J Neuroimmunol.* 223:55–64.

ANNALS of Clinical and Translational Neurology
Open Access
ANA American Neurological Association since 1875

RESEARCH ARTICLE

Dietary Yeasts Reduce Inflammation in Central Nerve System via Microflora

Kazushiro Takata[1], Takayuki Tomita[2], Tatsusada Okuno[1], Makoto Kinoshita[3,6], Toru Koda[1], Josephe A. Honorat[1], Masaya Takei[2], Kouichiro Hagihara[2], Tomoyuki Sugimoto[4], Hideki Mochizuki[1], Saburo Sakoda[5] & Yuji Nakatsuji[1]

[1]Department of Neurology, Osaka University Graduate School of Medicine D4, 2-2 Yamada-oka, Suita, Osaka, 565-0871, Japan
[2]Discovery Research Laboratories, Kyorin Pharmaceutical Co., ltd., 2399-1, Nogi, Nogi-machi, Shimotsuga-gun, Tochigi , 329-0114, Japan
[3]Laboratory of Immune Regulation, Department of Microbiology and Immunology, Osaka University Graduate School of Medicine C6, 2-2 Yamada-oka, Suita, Osaka, 565-0871, Japan
[4]Research Division, Hirosaki University Graduate School of Science and Technology, 3-bunkyocho, Hirosaki, Aomori, 036-8560, Japan
[5]Department of Neurology, National Hospital Organization Toneyama, 5-5-1 Toneyama, Toyonaka, Osaka, 560-8552, Japan

Correspondence
Yuji Nakatsuji, Department of Neurology Osaka University Graduate School of Medicine D4, 2-2 Yamada-oka, Suita, Osaka 565-0871, Japan. Tel: +81-6-6879-3571; Fax: +81-6-6879-3579; E-mail: yuji@neurol.med.osaka-u.ac.jp

Present address
[6]Current address: Osaka General Medical Center, 3-1-56, Mandaihigashi, Sumiyoshi, Osaka, Osaka, 558-0056, Japan

Funding Information
This study was supported by the Health and Labor Sciences Research Grants-in-Aid for Research on Intractable Diseases from the Ministry of Health, Labor and Welfare of Japan (ID:13277062), grants from the Health and Labor Sciences Research Grants from the Ministry of Health, Labor and Welfare of Japan and research support from Kyorin pharmaceutical Co., ltd.

Received: 22 July 2014; Revised: 28 October 2014; Accepted: 2 November 2014

Abstract

Objectives: The intestinal microflora affects the pathogenesis of several autoimmune diseases by influencing immune system function. Some bacteria, such as lactic acid bacteria, have been reported to have beneficial effects on immune function. However, little is known about the effects of yeasts. Here, we aimed to investigate the effects of various dietary yeasts contained in fermented foods on experimental autoimmune encephalomyelitis (EAE), an animal model of multiple sclerosis (MS), and to elucidate the mechanisms underlying these effects. **Methods:** The effects of eight yeasts selected from 18 types of yeasts contained in fermented foods were examined using an EAE model. Of these, *Candida kefyr* was investigated by analyzing the intestinal microflora and its effects on intestinal and systemic immune states. **Results:** Administration of *C. kefyr* ameliorated the severity of EAE. Reduced numbers of Th17 cells, suppressed interleukin (IL)-6 production by intestinal explants, and increased Tregs and CD103-positive regulatory dendritic cells in mesenteric lymph nodes (MLNs) were observed. Analysis of 16s-rDNA from feces of *C. kefyr*-treated mice demonstrated increased *Lactobacillales* and decreased *Bacteroides* compared to control flora. Transfer of intestinal microbiota also resulted in decreased *Bacteroides* and ameliorated symptoms of EAE. Thus, oral administration of *C. kefyr* ameliorated EAE by altering the microflora, accompanied by increased Tregs and CD103-positive regulatory dendritic cells in MLNs and decreased Th17 cells in the intestinal lamina propria. **Interpretation:** Oral ingestion of *C. kefyr* may have beneficial effects on MS by modifying microflora. In addition, our findings also suggested the potential health benefits of dietary yeasts.

doi: 10.1002/acn3.153

Introduction

Food habits and intestinal microflora have been shown to modulate the intestinal and systemic immune states, thereby affecting human health.[1,2] Th17 cells are induced by intestinal segmented filamentous bacteria and have been implicated in the pathogenesis of autoimmune diseases, including experimental autoimmune encephalomyelitis (EAE).[3–5] On the other hand, certain groups of commensal bacteria and their metabolites play critical roles in the induction of Foxp3-positive regulatory T cells in the colon.[6] Furthermore, the intestine itself has a mechanism to control excessive inflammation by eliminating or suppressing pro-inflammatory Th17 cells.[7]

These data highlight the importance of immune responses in the intestine.

Indeed, intestinal microflora and related intestinal immune mechanisms affect the susceptibility of humans and animals to inflammatory autoimmune diseases. For example, fermented foods and lactic acid bacteria are thought to have healthful effects, and recent studies have shown that modification of intestinal microflora ameliorates clinical symptoms of experimental disease models such as EAE and inflammatory bowel disease.[8,9] Although the effects of lactic acid bacteria on various autoimmune diseases have been reported,[10,11] few studies have investigated the effects of yeasts, such as *Saccharomyces*, *Candida*, and *Aspergillus* species, which are found in fermented foods.

Kefir is an acidic, mildly alcoholic fermented milk originating from the Caucasus mountains. Kefir grains represent a natural symbiosis of yeasts and lactic acid bacteria.[12] Importantly, in a mouse model of bronchial asthma, kefir has been reported to have anti-inflammatory and anti-allergic effects.[13]

In the current study, we sought to determine whether yeasts found in fermented foods have beneficial effects on EAE. Our results suggested that ingestion of *Candida kefyr*, one of the yeasts examined in this study, is a novel therapeutic strategy for overcoming autoimmune disease.

Materials and Methods

Reagents and animals

All yeasts (Table S1) were purchased from the National Institute of Technology and Evaluation (NITE) Biological Resource Center (NBRC, Chiba, Japan). They were cultured according to the manufacturer's protocols. The use of viable yeast is restricted in our animal facility because of the requirement for maintenance of specific pathogen-free conditions, yeasts were dissolved in 0.2 g/mL double distilled water (DDW), and all yeasts were heat-killed at 120°C for 15 min and stored at −80°C. C57BL/6 mice were administered water containing 8 mg/mL heat-killed yeasts in water bottles beginning at 14 days before immunization.

Induction of EAE

All experimental procedures were approved by the Animal Care and Use Committee of Osaka University Graduate School of Medicine. C57BL/6 mice were obtained from Oriental Yeast Corp. (Tokyo, Japan). EAE was induced as described previously.[10] In brief, after administration of heat-killed yeasts for 14 days, as described above, C57BL/6 mice were subcutaneously injected with 100 μg myelin oligodendrocyte glycoprotein (MOG) 35–55 (MEV GWYRSPFSPVVHLYRNGK) peptide ($MOG_{35–55}$) emulsified in complete Freund's adjuvant (CFA) containing 200 μg of *Mycobacterium tuberculosis* H37Ra (Difco Laboratories, Detroit, MI). Mice were concurrently injected twice with 200 ng of pertussis toxin (List Laboratories, Campbell, CA) on days 0 and 2. All mice were monitored daily for clinical signs and were scored as described previously.[10]

Histology and semiquantification of data

Mice were sacrificed on day 22 postimmunization followed by transcardiac perfusion with 4% paraformaldehyde in PBS. Spinal cords were fixed in 4% paraformaldehyde in PBS and prepared for histological analysis. Cryosections (10-μm thick) were stained with hematoxylin and eosin (H&E). Semiquantitative histological analysis of inflammatory cellular infiltration was performed as previously described.[14]

Isolation of MNCs and lymphocytes

MLNs, inguinal lymph nodes (ILNs), and cervical lymph nodes (CLNs) were harvested and homogenized. Cells were centrifuged and the resulting pellets were used as lymphocytes. Lamina propria (LP) lymphocytes were isolated as previously described.[10] The detailed method to isolate LP lymphocytes is described in the Data S1.

Cytokine assay

For the assessment of antigen-specific cytokine production, mononuclear cells (MNCs) were isolated from draining ILNs and cervical LNs of mice on day 8 after immunization with $MOG_{35–55}$. Cells were restimulated with the peptide for 72 h, and interleukin (IL)-17, interferon (IFN)-γ, and IL-10 were assayed by enzyme-linked immunosorbent assay (ELISA) according to the manufacturer's instructions (R&D Systems, Minneapolis, MN).

Intracellular cytokine staining

Intracellular expression of IL-17 and IFN-γ in $CD4^+$ T cells was analyzed using an Intracellular Fixation and Permeabilization Buffer Set (eBioscience, San Diego, CA) according to the manufacturer's instructions. Surface staining was performed with anti-CD4-APC-H7 antibodies (BD Biosciences, Franklin Lakes, NJ, USA). The cells were then stained with Fixable Viability Dye eFluor 450, fixed with fixation solution, and then washed with permeabilization diluent. Intracellular cytokine staining was performed with anti-IL-17A Alexa Fluor 647 (BD Biosciences), anti-IL-10-PE (BD Biosciences), and anti-IFN-γ-FITC (fluorescein isothiocyanate) (BioLegend,

San Diego, CA) antibodies. For intracellular staining of Foxp3, cells were stained using a Foxp3 Staining Buffer set (eBiosciences).

Flow cytometry

The following antibodies were used for flow cytometry: anti-CD4-APC/H7, anti-CD11c-PE/Cy7, anti-major histocompatibility complex (MHC) class II-Pacific Blue, and anti-CD103-APC antibodies (BD Biosciences). Anti-Foxp3-Alexa Fluor 647 antibodies (eBioscience) were also used; conditions were set according to the manufacturer's instructions. Data were acquired using a FACS Cant-2 instrument with Diva software (Becton Dickinson, Franklin Lakes, NJ, USA).

Intestinal tissue explant cultures

Explant culture was performed according to previously published methods with some modifications.[15,16] Briefly, large intestines were collected, opened longitudinally, washed in PBS to remove contents, and shaken at 110 rpm in RPMI 1640 containing 50 mg/mL gentamicin, 100 U/mL penicillin, 100 mg/mL streptomycin (GIBCO, Carlsbad, CA, USA), and 5 mmol/L ethylenediaminetetraacetic acid for 20 min at 37°C. After removing epithelial cells and fat tissue, intestinal tissue was cut into 10-mm fragments. Tissue fragments were incubated in 0.5 mL RPMI is abbreviation of Roswell Park Memorial Institute medium. Normally, RPMI is used. 1640 supplemented with 50 mg/mL gentamicin, 100 U/mL penicillin, 100 mg/mL streptomycin, and 5% heat-inactivated fetal bovine serum. Supernatants from the tissue fragment incubations were collected after 24 h for cytokine ELISAs (IL-6 and IL-10; R&D Systems), and tissue dry weights were measured.

Intestinal microflora analysis (T-RFLP method)

Analysis of intestinal bacterial flora using mouse fecal specimens was outsourced to Techno Suruga Laboratory (Shizuoka, Japan), where the T-RFLP (terminal restriction fragment length polymorphism) method was used.[17] The details of this method are described in the Data S1.

Microflora transfer

Microflora transfer was performed according to previously published methods, with modifications.[18] Briefly, 6-week-old female mice were treated with a cocktail of antibiotics (0.5 mg/mL vancomycin [Duchefa Biochemie, Haarlem, the Netherlands], 1 mg/mL ampicillin, 1 mg/mL metronidazole, 1 mg/mL neomycin, and 1 mg/mL gentamicin [Nacalai Tesque, Kyoto, Japan]) in drinking water for 2 weeks. Diluted cecal contents were collected from 8-week-old mice treated with *C. kefyr* or water for 2 weeks. The ceca of control mice or *C. kefyr*-treated mice were dissected and opened, and the contents were transferred to a sterile tube and resuspended in 50 volumes of sterile water. Next, 200 μL of this suspension was administered to each recipient by oral gavage using a gavage needle for five consecutive days. At 2 days after the final oral gavage, feces were collected for T-RFLP analysis, and mice were immunized for EAE.

Statistical analysis

Statistical analysis of the results was performed by one-way analysis of variance (ANOVA). Repeated measures ANOVA was used to compare the ratio of bacteria in T-RFLP analysis. Differences were considered significant when P values were less than 0.05. The data were analyzed using SPSS 14.J. (SPSS, Chicago, IL, USA)

Results

Candida kefyr decreased the susceptibility of mice to EAE

Eighteen types of yeasts that are found in common fermented foods were investigated in this study (Table S1). Because TNF-α is involved in the pathogenesis of intestinal autoimmune diseases[19,20] and IL-10 is a key anti-inflammatory cytokine involved in the maintenance of intestinal homeostasis,[21,22] the effects of yeasts on the production of these cytokines by MNCs from intestinal LP were examined. The yeasts were then classified into four groups depending on the pattern of relative cytokine production: high TNF-α/high IL-10, high TNF-α/low IL-10, low TNF-α/high IL-10, and low TNF-α/low IL-10 (data not shown). Eight yeasts representing the four groups were arbitrarily selected, and their effects on EAE model mice were examined. When administered beginning 14 days before immunization with MOG_{35-55}, only *C. kefyr*, which belonged to the low TNF-α/low IL-10 group, significantly ameliorated the clinical severity of EAE symptoms (Fig. 1A). Pathological examinations revealed that the number of infiltrated MNCs into the spinal cords of mice treated with *C. kefyr* was apparently lower than that observed in the control group (Fig. 1B). The significant decrease in the number of infiltrating cells in the *C. kefyr*-treated group was confirmed by semiquantitative analysis (*C. kefyr*: 1.16 ± 0.24 vs. control: 2.07 ± 0.22; $P = 0.010$; Fig. 1C). To investigate the effects of *C. kefyr* on systemic inflammation, draining inguinal LNs and cervical LNs harvested on day 8 after

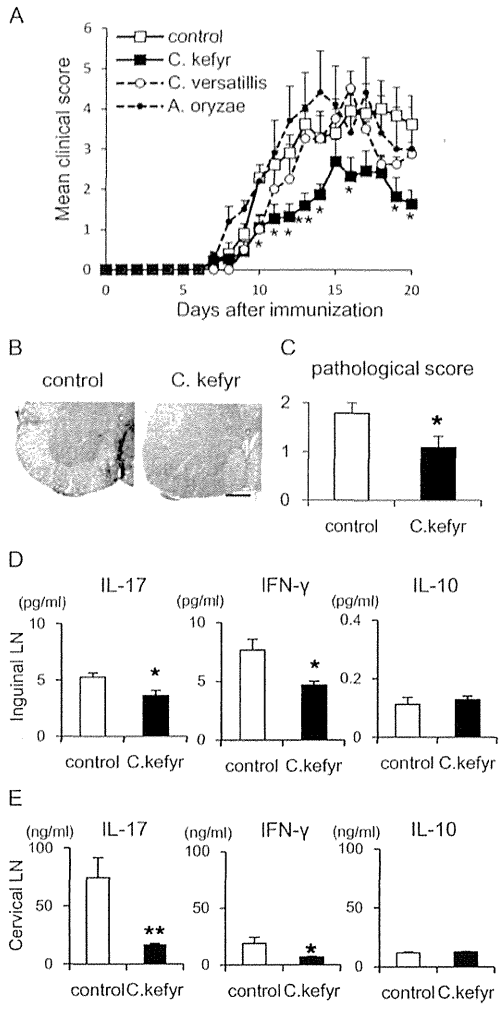

Figure 1. *Candida kefyr* ameliorates symptoms of EAE. The effects of *C. kefyr* (n = 11), *C. versatilis* (n = 8), *A. oryzae* (n = 6), and control (water, n = 9) on the clinical severity of EAE are shown. (A) The three yeasts listed above are shown because the other five yeasts did not differ significantly from the control. Yeasts were administered from 14 days before immunization until the end of the study. Data represent the mean clinical score +SEM. (*P < 0.05, **P < 0.01 compared to the control group using ANOVA). (B) Spinal cord sections obtained from control or *C. kefyr*-treated C57BL/6 mice on day 22 after immunization were analyzed by hematoxylin and eosin (H&E) staining. Scale bar = 250 μm. (C) Semiquantitative evaluation of the pathological scores was performed as described in the Materials and Methods section. Each bar indicates the mean pathological score +SEM of six mice from each group. Lymphocytes were isolated from draining lymph nodes (D) and cervical lymph nodes (E) on day 8 after immunization and then restimulated with MOG_{35-55} for 72 h. IL-17, IFN-γ, and IL-10 in the culture supernatants were assayed by ELISA. Data are means + SEMs and are representative of three independent experiments (n = 5–8 each). EAE, experimental autoimmune encephalomyelitis; ANOVA, analysis of variance; MOG, myelin oligodendrocyte glycoprotein; IL, interleukin; IFN, interferon; ELISA, enzyme-linked immunosorbent assay.

immunization were restimulated with MOG_{35-55}. Both inguinal and cervical LNs obtained from the *C. kefyr*-treated mice produced significantly less IL-17 and IFN-γ than those obtained from the control group. The production of IL-10 did not differ significantly between the two groups (Fig. 1D and E). Although we assayed IL-4 to examine the effects of *C. kefyr* on Th2-skewing, the levels were below the sensitivity of the assay system. These data suggested that treatment with *C. kefyr* inhibited the induction of antigen-specific Th17 and Th1 cells.

Next, the effects of *C. kefyr* were examined in a model of dextran sulfate sodium (DSS)-induced colitis because inflammatory bowel disease is known to be directly affected by intestinal microflora and intestinal immunity.[23] In this colitis model, prophylactic oral administration of *C. kefyr* significantly inhibited body weight loss, reduced colon length, and increased relative colon weights (Fig. S1A–D). The effects of other *Candida* species were less prominent than those of *C. kefyr*, and no significant differences were observed compared to the control. The effects of *C. kefyr* were also examined in a toluene-2, 4-diisocyanate (TDI) contact dermatitis model, another model of autoimmune dysfunction. However, *C. kefyr*, as well as the other yeasts examined (*C. versatilis*, *C. valida*, and *Saccharomyces cerevisiae*), had no effects on TDI-induced dermatitis (Fig. S2). Thus, our data supported that *C. kefyr* ameliorated symptoms of EAE and DSS-induced colitis, but did not affect TDI-induced dermatitis, suggesting that the efficacy was disease specific.

When *C. kefyr* administration was initiated on day 8 after immunization of mice with EAE, clinical severity was not affected (Fig. S3A). Moreover, in the DSS-induced colitis model, disease deterioration was observed when *C. kefyr* was administered after DSS induction (data not shown). Thus, *C. kefyr* was not effective as a therapeutic agent, but exhibited efficacy in the prophylactic/preventive setting.

Candida kefyr suppressed generation of Th17 cells and induced production of regulatory T cells (Tregs) and dendritic cells

In order to elucidate the mechanism through which *C. kefyr* suppressed intestinal and systemic inflammation, we analyzed $CD4^+$ T cells from mice treated with *C. kefyr*. Intracellular staining of $CD4^+$ T cells from LP and MLNs of mice treated with *C. kefyr* for 2 weeks revealed that $CD4^+$ IL-17-producing cells were downregulated in intestinal LP in both small and large intestines (Fig. 2A). The production of IL-6 by intestinal tissue explants was also downregulated in both small and large intestines, and IL-10 was significantly upregulated in the colon (Fig. 2B). Significantly increased percentages of $CD4^+$ $Foxp3^+$ iTregs

